"Simulation and Control of Doubly-Fed Induction Generator"

By

Chirag Vadaliya

12MEEP29

DEPARTMENT OF ELECTRICAL ENGINEERING

AHMEDABAD-382481

May 2014

"Simulation and Control of Doubly-Fed Induction Generator"

Major Project Report

Submitted in Partial Fulfillment of the Requirements for the degree of

MASTERS OF TECHNOLOGY

IN

ELECTRICAL ENGINEERING
(Power Electronics, Machines & Drives)

By

Chirag Vadaliya
(12MEEP29)

Department of Electrical Engineering
INSTITUTE OF TECHNOLOGY
NIRMA UNIVERSITY
AHMEDABAD 382 481

May 2014

Undertaking for Originality of the Work

I **Chirag Vadaliya**, Roll No. **12MEEP29**, give undertaking that the Major Project entitled **"Simulation and Control of Doubly-Fed Induction Generator"** submitted by me, towards the partial fulfillment of the requirements for the degree of Master of Technology in **Power Electronics Machines** & **Drives, Electrical Engineering**, under Institute of Technology of Nirma University, Ahmedabad, is the original work carried out by me and I give assurance that no attempt of plagiarism has been made. I understand that in the event of any similarity found subsequently with any published work or any dissertation work elsewhere; it will result in severe disciplinary action.

....

Signature of Student

Date:

Place:

Endorsed by:

....

(Signature of Project Guide)

Prof. Amit N Patel

Assistant Professor

Department of Electrical Engineering

Institute of Technology

Nirma University

Ahmedabad

CERTIFICATE

This is to certify that the Major Project Report entitled **"Simulation and Control of Doubly-Fed Induction Generator"** submitted by **Mr. Chirag Vadaliya** (**Roll No.: 12MEEP29**) towards the partial fulfillment of the requirements for Master of Technology (Electrical Engineering) in the field of Power Electronics, Machines & Drives of Nirma University is the record of work carried out by him under our supervision and guidance. The work submitted has in our opinion reached a level required for being accepted for examination. The results embodied in this major project work to the best of our knowledge have not been submitted to any other University or Institution for award of any degree or diploma.

Date:

....

Industry Guide

Mr. Vinod Patel

AGM,R&D Department
Amtech Electronics (India) Ltd.
Gandhinagar.

....

Institute Guide

Prof. Amit N.Patel

Department of Electrical Engineering
Institute of Technology
Nirma University
Ahmedabad.

Head of Department

Department of Electrical Engineering
Institute of Technology
Nirma University
Ahmedabad

Director

Institute of Technology
Nirma University
Ahmedabad

Acknowledgement

First of all, I would like to thank AMTECH Electronics (I) Ltd., Gandhinagar, for giving me an opportunity to perform the project under its premises and give me the industrial exposure.

I wish to express my sincere gratitude to Mr. Vinod Patel, AGM, *R&D* department, AMTECH Electronics (I) Ltd., Gandhinagar, for his guidance and support. His technical expertise and vast experience has always helps me to find technical solutions to realistic problems. He always helped me and encouraged me throughout the period we have worked together. I also like to thank to Mr. Anupsingh Chandel for showing interest in the project and giving me suggestion for improving this work.

I like to thank my institute guide Mr. Amit N Patel (Assistant professor, Nirma University) co-guide Mr. T.H.Panchal (Section Head, EE Dept.) for providing many insightful comments and constructive suggestion in every reviews of my dissertation.

I am thankful to Dr. P.N.Tekwani (HOD, EE Dept.) for allowing me to do my project work at AMTECH Electronics (I) Ltd., Gandhinagar. I would also like to thank Mr. P.N.Kapil (Assistant professor, EE Dept.) for showing interest in the project and for giving valuable suggestion for improving this work.

Further I am thankful to all colleagues for their continuous support during my project work.
Special thanks to my parents and my family members for their continuous support and encouragement.

Chirag M Vadaliya

Abstract

Wind energy plays an increasingly important role in the world because it is friendly to the environment. During the last decades, the concept of a variable-speed wind turbine (WT) has been receiving increasing attention due to the fact that it is more controllable and efficient, and has good power quality. As the demand of controllability of variable speed WTs increases, it is therefore important and necessary to investigate the modeling for wind turbine-generator systems (WTGS) that are capable of accurately simulating the behavior of each component in the WTGS. Therefore, the main focus will be on models of a grid-connected wind turbine system equipped with a 2MW/690 V doubly-fed induction generator (DFIG), which includes back-to-back power converter. In order to obtain satisfying output power from the WTGS, control strategies are also necessary to be developed. These control schemes include the grid-side converter control, the generator-side converter control. The grid-side converter controller is used to keep the DC-link voltage constant and yield a unity power factor looking into the WTGS from the grid-side. The generator-side converter controller has the ability of regulating the torque, active power and reactive power. Vector control scheme is used to control back-to-back PWM converters. The simulation verification of system will be performed in PSIM software.

List of Figures

List of Tables

Abbreviations

BDIG .... Brush-less doubly fed induction generator
DFIG .... Doubly-fed induction generator
DFIM .... Doubly-fed induction machine
emf .... electromotive force
GSC .... Grid side converter
IEEE .... Institute of Electrical and Electronic Engineers
K.E. .... Kinetic energy
MPPT .... Maximum Power Point Tracking
PMSG .... permanent magnet synchronous generator
PWM .... Pulse Width Modulation
RSC .... Rotor side converter
SCIG .... Squirrel-cage induction generator
TSR .... Tip-speed ratio
WECS .... Wind Energy conversion system
WRIG .... Wound-rotor induction generator

Nomenclature

m .... mass of air

V .... Velocity of air

ρ .... air density

A .... Rotor swept area

C_p .... Power coefficient

P_{out} .... output power

P_{air} .... Power in moving air

λ .... Tip speed ratio

θ .... Pitch angle

D .... Diameter of rotor blades

n .... number of blades

$T_{turbine}$ .... Wind turbine torque

ω_r .... rotor speed

ω_e .... synchronous speed

V_a, V_b, V_c .... terminal voltage of stator

V_{ar}, V_{br}, V_{cr} .... terminal voltage of rotor

I_a, I_b, I_c .... stator phase current

I_{ar}, I_{br}, I_{cr} .... rotor phase current

R_s .... resistance of stator phase winding

R_r .... resistance of rotor phase winding

L_s .... self inductance of stator phase winding

L_r .... self inductance of rotor phase winding

L_{ls} .... leakage inductance of stator phase winding

L_{lr} .... leakage inductance of rotor phase winding

L_m .... magnetizing inductance

ψ_a, ψ_b, ψ_c .... stator flux linkage

ψ_{ar}, ψ_{br}, ψ_{cr} .... rotor flux linkage

V_{qs}, V_{ds} .... stator terminal voltage expressed in d-q synchronous reference frame

V_{qr}, V_{dr} .... rotor terminal voltage expressed in d-q synchronous reference frame

ψ_{ds}, ψ_{qs} .... stator flux linkage in d-q reference frame

ψ_{dr}, ψ_{qr} .... rotor flux linkage in d-q reference frame

I_{qs},I_{ds} .... stator current in d-q reference frame

I_{qr},I_{dr} .... rotor current in d-q reference frame

$\psi_{s\alpha}$, $\psi_{s\beta}$ .... flux linkage of stator in α-β coordinates

I_{ms} .... magnetizing current

$|\psi_s|$ .... magnitude of stator flux linkage

$I_{s\alpha}$, $I_{s\beta}$ .... statorα-β axes current

$I_{r\alpha}$, $I_{r\beta}$ .... rotorα-β axes current

$|V_s|$ .... magnitude of stator voltage

θ_s .... stator flux angular position

θ_e .... angular position of supply voltage

θ_{er} .... rotor electrical position

P .... number of pole

p_1 .... number of pole pair

V_{dc} .... dc-link voltage

I_{dc} .... dc-link current

P_s .... active power of stator

Q_s .... reactive power of rotor

P_r .... active power of rotor

P_r .... ractive power of rotor

Contents

Chapter 1

INTRODUCTION

1.1 General

In recent years, the environmental pollution has become a major concern in people's daily life and a possible energy crisis has lead people to develop new technologies for generating clean and renewable energy. Wind power along with solar energy, hydropower and tidal energy are possible solutions for an environmentally-friendly energy production. Among these renewable energy sources, wind power has the fastest growing speed (approximately 20% annually) in the power industry. The large increasing electrical penetration of large wind turbines into electrical power systems is inspiring continuously the designers to develop both custom generators and power electronics, and to implement modern control strategies.

The continued growth and expansion of the wind power industry in the face of a global recession and a financial crisis is a testament to the inherent attractiveness of the technology. wind power is clean, reliable, and quick to install; it's the leading electricity generation technology in the fight against climate change, enhancing energy security, stabilizing electricity prices. Until late 1990s, most wind turbine manufacturers built constant speed wind turbines with power levels below 1.5 MW using a multi-stage gearbox and a standard squirrel cage induction generator.

Nowadays, most wind turbine manufacturers have changed to variable speed wind turbines for power levels from roughly 1.5 to 5 MW. They have used a multi-stage gearbox, a relatively low cost standard doubly fed induction generator and a power electronic converter feeding the rotor winding with a power rating of approximately 30% of the rated power of the turbine.

However, since 1991s, there have also been wind turbine manufacturers proposing gearless generator system with so called direct-drive generators, mainly to reduce failures in gearboxes and to lower maintenance problems. But power electronic converter needed for this is of full rated power as compared to DFIG, which requires power converter of rating 30% of full rated power. For the increasing power levels and decreasing speeds, these direct-drive generators are become larger and even more expensive. Therefore, it has been proposed to use a single-stage gearbox and doubly fed induction generators.

1.2 Wind energy present scenario

As per Global Wind Energy Council report of 2013[1], The recent strong growth in new technologies for wind power and solar photo voltaic has created expectations among policy makers and the industry alike that these technologies will make a major contribution to meet growing electricity needs in the near future.

As shown in figure 1.2, The new global total at the end of 2013 was 318.1 GW, representing cumulative market growth of more than 19%, an excellent industry growth rate given the economic climate, even though it is lower than the annual average growth rate over the last 10 years of about 22%. The market for new wind turbines reached a new record: 44,799 Megawatt were installed in 2012, an increase of 12 %

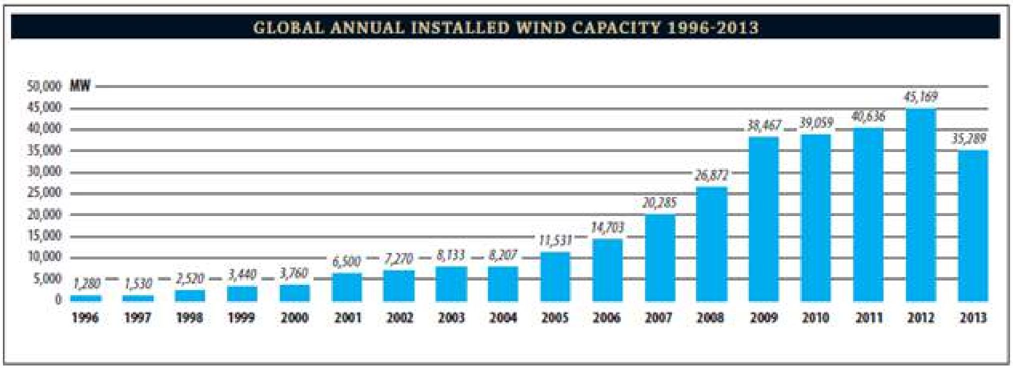

Figure 1.1: Global annual installed wind capacity 1996-2013

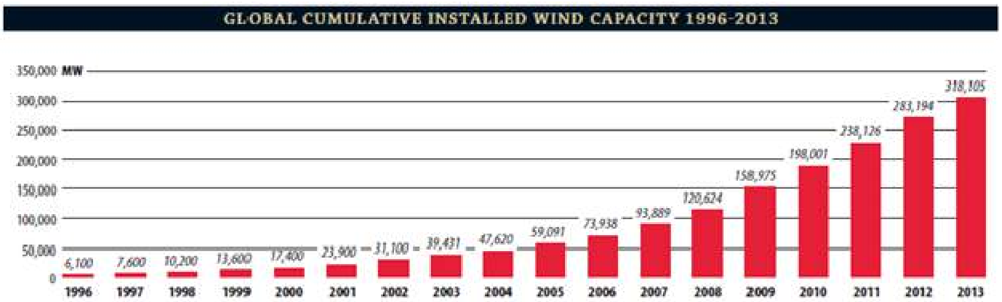

Figure 1.2: Global cumulative installed wind capacity 1996-2013

compared with 2011 when 40,561 Megawatt were erected. the 35,289 Megawatt is erected in the year of 2013.

Table I shows the top ten countries of wind power capacity. India was the second country in Asia to develop wind power on a commercial scale. China is major contributor in wind power generation capacity. the installed capacity in the China is 15,860 MW in the year of 2013 and their total installed wind power capacity is 91,424 MW at the end of year 2013. The wind power capacity installed in India in the year of 2013 is 1,729 MW, and their total wind power capacity is 20,150 MW at the end of year 2013. World's top ten countries of wind power generation capacity are shown in fig. 1.3. Where, India is one of the countries of the world with most wind power on line, at number five.

Table I: Top ten countries of wind power capacity

country	**Total capacity end 2013(MW)**
China	91,424
United State	61,091
Germany	34,250
Spain	22,959
India	20,150
United Kingdom	10,531
Italy	8,525
France	8,254
Canada	7,803
Denmark	4,772
Rest of world	48,351
Total	**318,137**

Table II: State-wise installed capacity in India

State	**Capacity as on 31-03-2013 (MW)**
Tamil Nadu	7162.18
Gujarat	3174.58
Maharastra	3021.85
Rajasthan	2684.65
Karnataka	2135.50
Andhra Pradesh	447.65
Madhya Pradesh	386.00
Kerala	35.10
Others	4.30
Total	**19051.46**

In India, Tamil Nadu is major contributor,which contributes 37.59% of total wind power capacity of India. The State-wise contribution of wind power capacity in India is Shown in Table II.

1.3 Problem Formulation

The amount of wind energy supplied to the electrical network is considerably increasing, therefore having an efficient and a reliable control system is very important. There are two type of wind energy conversion systems, 1). fixed-speed 2). variable speed. Fixed-speed wind energy conversion system has disadvantages that the turbulence of the wind will result in power variations, and thus affect the power quality of the grid where as in a variable-speed wind turbine the generator is controlled by power electronic equipment, which makes it possible to control the rotor speed. In this way the power fluctuations caused by wind variations can be more or less absorbed by changing the rotor speed and thus power variations originating from the wind conversion and the drive train can be reduced. Hence, the power quality impact caused by the wind turbine can be improved compared to a fixed-speed turbine.

PMSG and DFIG is used for variable speed energy conversion system. In WECS with PMSG is consist of back to back PWM converters, DC link and grid. Advantages of this WECS is there is no need of gearbox, wind turbine is directly connected to the PMSG. So the maintenance of gearbox is not required, high efficiency and reliable, smaller in size and easy to control. But the back to back converter should be rated at full-Scale of power which increases the cost of converter and the whole system.

In DFIG wind energy conversion system, the stator of generator is directly connected to the grid and the rotor is connected to the grid via back to back PWM converter a generator side converter and grid side converter. The grid side converter control the power flow in order to keep the DC-link voltage constant, while the generator side converter controls the torque and speed. The rotor supplies the slip power to the grid so the converter is rated only slip power. General representation of DFIG base wind energy conversion system is shown in figure 1.3

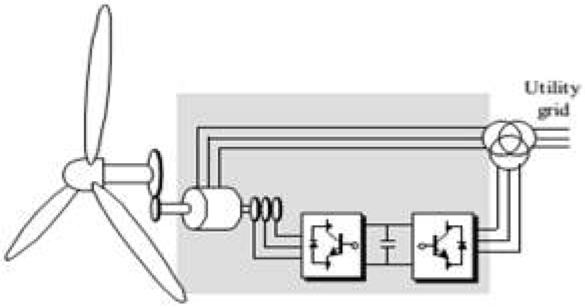

Figure 1.3: Representation of DFIG based WECS

One of the important Advantage of DFIG system is cost of converter is less because converter rating typically 30% of total power of system, limitation of this system is it use slip ring and gearbox which require periodic maintenance and has complex control scheme.

1.4 Scope of work

The amount of wind energy supplied to the electrical network is considerably increasing, therefore having an efficient and a reliable control system is very important. Modeling the power system and performing the simulation helps to have a better understanding of the system.

The main focus is given to implementation and control of 2 MW/690 V DFIG and designing generator side converter using stator flux oriented vector control technique to control active and reactive power control or torque and speed and the designing source side converter to control the DC link voltage and to control reactive power for unity power factor operation.

1.5 Literature Survey

With the concern of environmental pollution wind power being established in many countries. Wind power has the fastest growing speed approximately 20% annually in power industry [1]. Detailed analysis of global wind energy production, and the top-ten wind energy country is given in [2]. DFIM using an AC-AC converter in the rotor circuit (Schrebius drive) has long been a standard drive option for high power applications involving a limited speed range. The power converters only handle the rotor power [3]. The advantages of variable-speed wind turbine over fixed-speed wind turbine 1) Annual energy production is increase 2)power quality can be improved by reducing power pulsation 3)mechanical stress on turbine blade is reduced is given in [4]. While, in [5], it states that the increase in energy production can be 39% with the use of variable-speed wind turbine. In [6], it shown that, the gain in energy generation of the variable-speed wind turbine compared to the most simple fixed-speed wind turbine can vary between 3-28% depending on the site condition. The different topology of wind energy conversion system to capture wind power is shown in [7]. According to [7], the wind energy capture can be significantly increased by using DFIG. They also state an increased energy capture of a DFIG by over 20% with respect to a variable-speed system using a cage bar induction machine and by over 60% in comparison to a fixed-speed systems. it also state that the power electronic converter have to handle only a fraction of the total power of the system so, converter cost is less. The study of DFIG based wind turbine is given in [8]. The mathematical modelling of DFIG is given in [9] [10]. Control of DFIG is more complicated than the control of a standard induction machine. In order to control the DFIG the rotor current is controlled by a power electronics converter. One common way of controlling the rotor current is by mean of field-oriented (vector) control. One common way is to control the rotor current with stator-flux orientation [11][12][13][14]. The MPPT affects the efficiency of generator connected to the grid. the MPPT algorithm for DFIG based wind turbine system is explained in [15]. The Rotor side converter is used to control the active and reactive power and hence, torque while, the Grid side converter is used to maintain the DC-link constant and unity power factor at grid side with the use of vector control scheme [16][17].

Chapter 2

BASIC OF WIND ENERGY CONVERSION SYSTEM

2.1 Basic concept of Wind turbine

A wind energy conversion system transforms wind kinetic energy to mechanical energy by using rotor blades. This energy is then transformed into electric energy by a generator. The system is made up of several components, participating directly in the energy conversion process.

- wind energy conversion system consists of:
  - Wind turbine
  - Generator
  - Gearbox
  - Generator control (converter)
  - DC link
  - Inverter
  - Transformer
  - Grid connection

2.1.1 Parts of Wind turbine

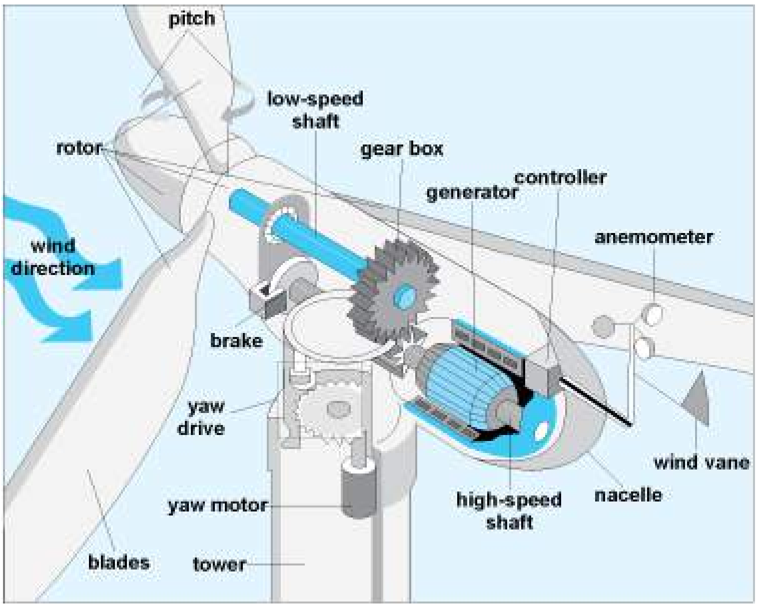

Figure 2.1: Components of a wind turbine-generator system

- Different parts:

Anemometer :

Measures the wind speed and transmit wind speed data to the controller.

Blades :

Most turbine have either two or three blades. Wind blowing over the blades causes the blade to lift and rotate.

Gearbox :

A gearbox is normally required to match the speed difference between the turbine and generator such that the generator can deliver its rated power at the rated wind speed.

Generator :

Wind turbine is a rotating machine, which converts the kinetic energy in the wind into mechanical energy. The mechanical energy is then converted to electricity, the machine is called a wind generator.

Brake :

A disc brake which can be applied mechanically, electrically, of hydraulically to stop the rotor emergencies.

Wind vane :

Measures wind direction and communicates with the yaw drive to orient the turbine properly with respect to the wind.

Yaw drive :

Upwind turbine face into the wind; the yaw drive used to keep the rotor facing into the wind as the wind direction changes. Downwind turbines don't require a yaw drive, the wind blows the rotor downwind.

Yaw motor :

Powers the yaw drive.

2.1.2 How wind turbine generates electrical power

- The wind strikes the wind turbine blades, causes them to spin and further makes the low-speed shaft rotate.
- The rotating low-speed shaft transfers the kinetic energy to the gearbox, which has the function of stepping up the rotational speed and rotating the high-speed shaft.
- The high-speed shaft causes the generator to spin at high speed which is close to the rated speed of the generator.
- The rotating generator converts the mechanical power to electrical power.

2.2 Wind speed and energy

The wind turbine captures wind's kinetic energy in a rotor consisting of two or more blades mechanically coupled to the electrical generators.

The kinetic energy in air of mass m moving with speed V is given by following equation in joules:

$$K.E. = \frac{1}{2} * m * V^2 \tag{2.1}$$

The power in mowing air is the flow rate of kinetic energy per second in watts:

$$P_{air} = \frac{1}{2} * \textit{(mass flow per second)} * V^2 \tag{2.2}$$

Then, the mass flow rate of the air in kilograms per second is ρAV.
The mechanical power coming in the upstram wind is given by the following in watts:

$$P_{air} = \frac{1}{2} * (\rho AV) * V^2 \tag{2.3}$$

$$P_{air} = \frac{1}{2} * (\rho A) * V^3 \tag{2.4}$$

Where,

$$A = \frac{\pi}{4} * D^2 \tag{2.5}$$

It is clear from equation 2.4 that, the wind power is proportional to the cube of wind speed if the diameter of blade is constant.
Output power from the wind turbine is,

$$P_{out} = \frac{1}{2} * \rho A * V^3 * C_p \tag{2.6}$$

Where, C_p is **power coefficient**, it gives the fraction of kinetic energy that is converted into mechanical energy by wind turbine. Maximum value of C_p is defined by Betz limit, which state that the turbine can never extract more than 59.3% of the power from the air. In reality, wind turbine rotors have maximum C_p values in the range of 25-45%.

Betz limit

The maximum fraction of the power in the wind that can theoretically be extracted by a wind power plant, usually given as 59.3%.

It is a function of the tip speed ratio λ and depends on the blade pitch angle θ for pitch-controlled turbine.

$$C_p = 0.22(\frac{116}{\beta} - 0.4\theta - 5)e^{\frac{-112}{\beta}} \tag{2.7}$$

Where,

$$\beta = \frac{1}{\frac{1}{\lambda+0.08\theta} - \frac{0.035}{\theta^3+1}} \tag{2.8}$$

Tip Speed Ratio

It is an extremely important factor in wind turbine design. TSR refers the ration between the outer tip of blade is moving divided by the wind speed:

$$TSR = \frac{rotortipspeed}{windspeed} \tag{2.9}$$

$$= \frac{rpm * \pi D}{60 * V} \tag{2.10}$$

The power coefficient, C_p, as a function of the tip speed ratio λ and pitch angle θ is shown in figure 2.2.

output torque

There is a direct relationship exists between power and torque and it is given by,

$$T_t = \frac{P_{out}}{\omega_t} \tag{2.11}$$

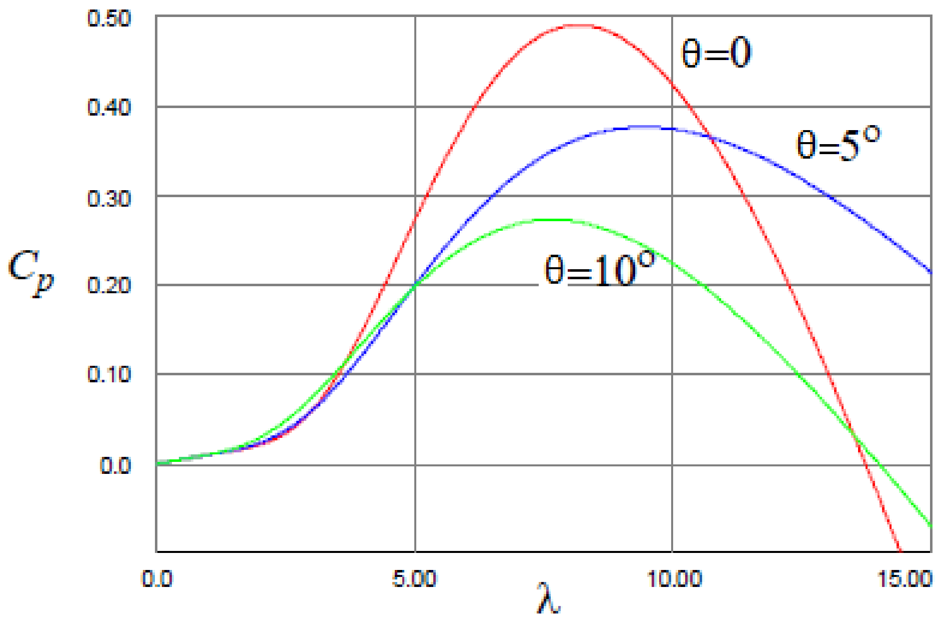

Figure 2.2: C_p vs λ

Using the optimum value of C_p and λ the value of aerodynamic torque can be expressed as

$$T_t = \frac{\rho \pi R^5 * C_{Pmax} * {\omega_t}^2}{2{\lambda_{opt}}^3} \tag{2.12}$$

2.3 Operating region of variable-speed wind turbine-generator system

The wind turbine always operates with different dynamics, from minimum wind speed to maximum wind speed, and the operating regions of the wind turbine can be illustrated by their power curve shown as in below figure 2.3

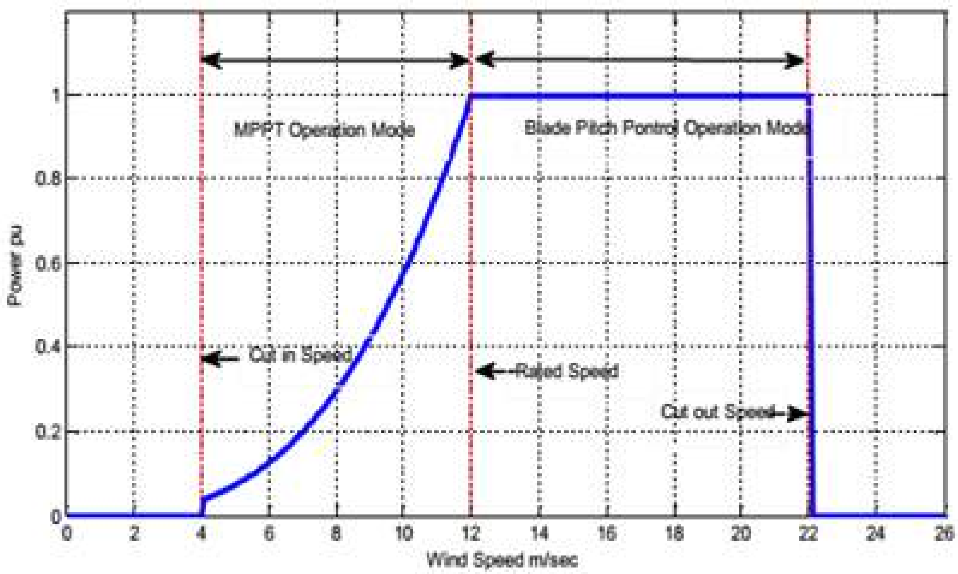

Figure 2.3: Power vs wind speed curve

- **Cut-In speed:**
  - The cut-in speed is the minimum wind speed at which the wind turbine will generate usable power. This wind speed is typically between 3.13 and 4.47 m/sec for most turbines.
- **Rated speed:**
  - The rated speed is the minimum wind speed at which the wind turbine will generate its designated rated power. At wind speeds between the cut-in speed and the rated speed, the wind turbine will operate at the maximum power point tracking (MPPT) mode, and the output power of a wind turbine will increase as the wind speed increases.
- **Cut-out speed:**
  - At very high wind speeds, typically between 22 and 45 m/sec, most wind

turbines cease power generation and are shut down for protection purposes. The wind speed at which shut down operation occurs is called the cut-out speed. When the wind turbine experiences high wind speed, the mechanical part of the wind turbine may be damaged, and hence having a cut-out speed is a safety consideration. When the wind speed drops back to a safety level, the wind turbine operation usually resumes.

In the MPPT operation mode, The control of a variable-speed wind turbine below the rated wind speed is achieved by controlling the generator. The main goal is to maximize the wind power capture at different wind speeds, which can achieved by adjusting the turbine speed in such a way that the optimal tip speed ratio λ_{opti} is maintained. The relations between the mechanical power, speed, and torque of a wind turbine can be used to determine the optimal speed or torque reference to control the generator and achieve the MPPT operation.

$$P_{mppt} = \frac{\rho \pi R^5 * C_{Pmax} * {\omega_t}^3}{2{\lambda_{opt}}^3} \tag{2.13}$$

Equation 2.13 shows the maximum power obtained using the strategy MPPT, which permit to adjust automatically the ratio speed at its optimum value (8.18) in order to obtain the maximum power coefficient C_{Pmax} (0.49)

In the blade pitch control operation mode, if the wind speed exceeds its rated value, it would be detrimental for the wind turbine to operate at such high wind speed. Hence, the generator speed must be limited by reducing the aerodynamic torque. This can be done through regulating the pitch angle of the blades, so that the aerodynamic conversion efficiency is reduced, and thus less mechanical torque acts on the generator, and finally the speed can be maintained at a constant level.

2.4 Types of Wind Energy Conversion Systems

According to the wind generator and wind turbine topologies, the WECS divides into four types;

- Fixed speed wind turbine (Type-A).
- Partial variable speed wind turbine with variable rotor resistance (Type-B).
- Variable speed wind turbines with partial scale power converter (Type-C).
- Variable Speed Wind Turbine with Full-Scale Power Converter (Type-D).

2.4.1 Fixed-speed wind turbine (Type-A)

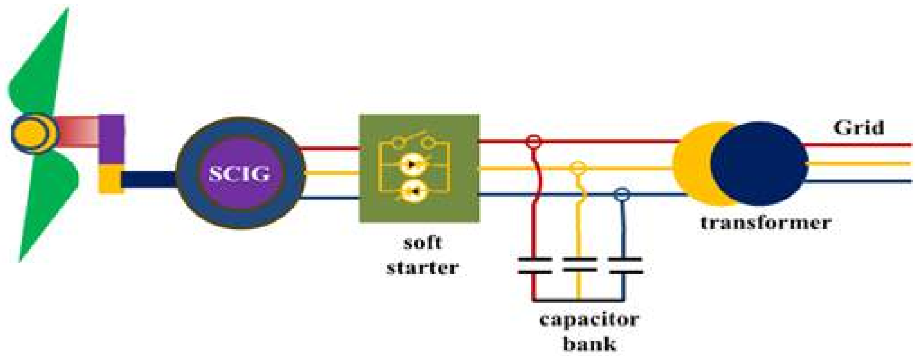

Figure 2.4: Power schematic of Fixed-speed WECS

Fixed-speed WECS operates at constant speed. That means, regardless of the wind speed, the wind turbine rotor speed is fixed and determined by the grid frequency. Fixed-speed WECS are typically equipped with squirrel-cage induction generator (SCIG), soft starter and capacitor bank and they are connected directly to the grid, as shown in figure. Fixed-speed WECS have the advantages of being simple, robust and reliable with simple and inexpensive electrical system. In this WECS the rotational speed of wind turbine can not be regulated and only vary with the wind speed.

2.4.2 Partial variable speed wind turbine with variable rotor resistance (Type-B)

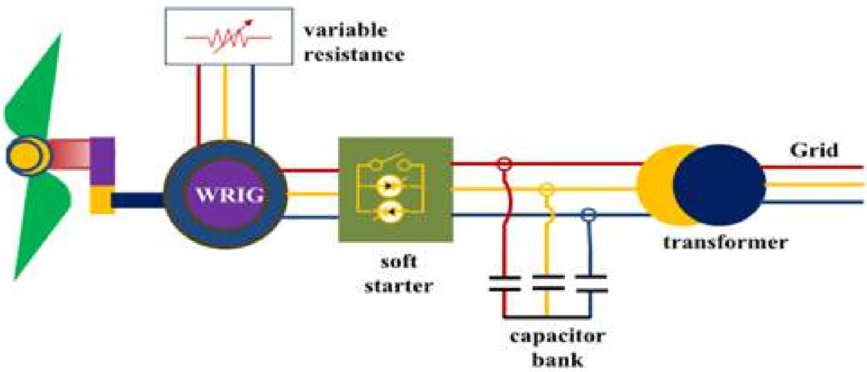

Figure 2.5: Power schematic of Partial Variable-speed WECS

This configuration corresponds to the limited variable speed wind turbine with variable generator rotor resistance. It uses a wound rotor induction generator (WRIG) and has been used. The generator is directly connected to the grid. A capacitor bank performs the reactive power compensation. A smoother grid connection is achieved by using a soft-starter. The unique feature of this concept is that it has a variable additional rotor resistance, which can be changed by an optically controlled converter mounted on the rotor shaft. This optical coupling eliminates the need for costly slip rings that need brushes and maintenance. The rotor resistance can be changed and thus controls the slip. This way, the power output in the system is controlled. The range of the dynamic speed control depends on the size of the variable rotor resistance. Typically, the speed range is 0 to 10% above synchronous speed. The energy coming from the external power conversion unit is dumped as heat loss.

2.4.3 Variable speed wind turbines with partial scale power converter (Type-C)

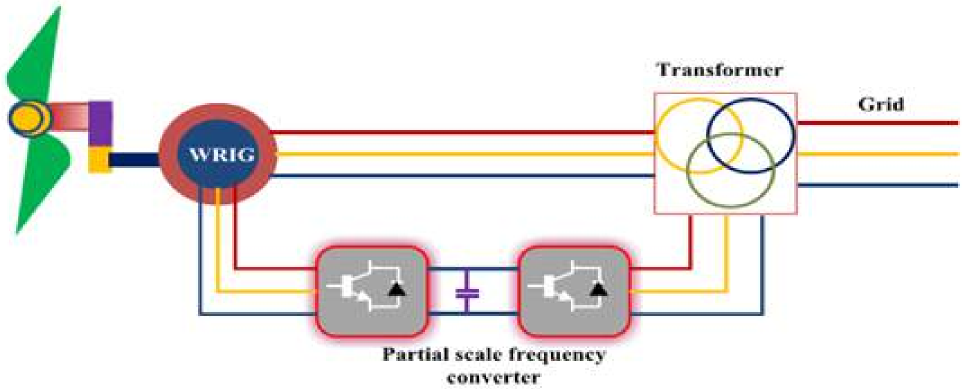

Figure 2.6: Power schematic of Variable-speed WECS with partial scale power converter

Variable speed wind turbines are currently the most used WECS. This configuration, known as DFIG based wind turbine, corresponds to the limited variable speed wind turbine with a WRIG and partial scale frequency converter (rated at approximately 30% of nominal generator power) on the rotor circuit. The partial scale frequency converter performs the reactive power compensation and the smoother grid connection. It has a wider range of dynamic speed control compared with that of second type of wind turbine, depending on the size of the frequency converter. Typically, the speed range comprises synchronous speed -30% to +30%. The smaller frequency converter makes this concept attractive from an economical point of view. so, this type of WECS is most used in wind power industry (around 50%).

2.4.4 Variable Speed Wind Turbine with Full-Scale Power Converter (Type-D)

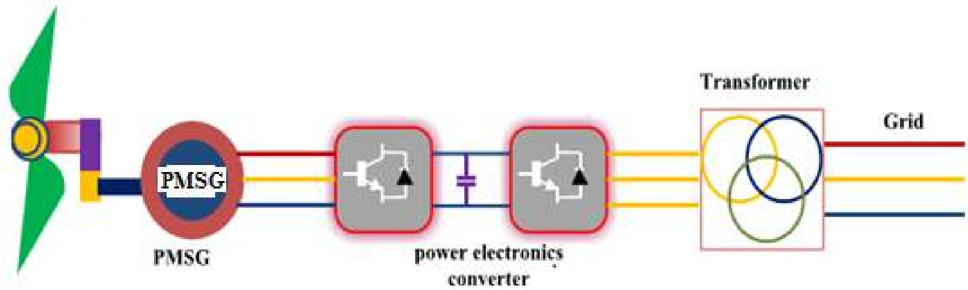

Figure 2.7: Power schematic of Variable-speed WECS with full-scale power converter

This configuration corresponds to the full variable speed wind turbine, with the generator connected to the grid through a full-scale frequency converter. The frequency converter performs the reactive power compensation and the smoother grid connection. The generator can be excited electrically (WRSG/WRIG) or by a permanent magnet (PMSG). Some full variable-speed wind turbine systems have no gearbox. In these cases, a direct driven multi pole generator with a large diameter is used. The disadvantages of this WECS is higher cost of converter due to full-Scale power converter.

2.5 Advantages of variable-speed WECS

- The annual energy production (AEP) increases because the turbine speed can be adjusted as a function of wind speed to maximize output power. Depending on the turbine aerodynamics and wind regime, the turbine will on average collect up to 10% more annual energy[4].

- Power quality can be improved by reduction the power pulsations. The reduction in the power pulsation results decreases voltage deviations from its rated value. This allows increasing the penetration of the wind power in network.

- The output power variation is decoupled from the instantaneous condition present in the wind and mechanical systems. When a gust of the wind arrives at the turbine, the electrical system can continue delivering constant power to the network while the inertia of mechanical system absorbs the surplus energy by increasing rotor speed.

- The mechanical stresses are reduced due to the compliance to the power train. The turbulence and wind shear can be absorbed, i.e. the energy is stored in the mechanical inertia of the turbine, creating a compliance that reduces the torque pulsation.

- Acoustic noises are reduced. The acoustic noise may be important factor when sitting new wind farms near populated areas.

- The pitch control complexity can be reduced. This is because the pitch control time constant can be longer with variable speed.

Although the main disadvantages of the variable-speed configuration are the additional cost and the complexity of power converters required to interface the generator and the grid, its use has been increased due to the above mentioned advantages.

Chapter 3

Doubly-Fed Induction Generator

3.1 Introduction

The function of blades is to convert kinetic energy in the wind into rotating shaft power to spin a generator that produces electric power. Generator consist of a rotor rotating of a rotor that spins inside of a stationary housing called stator. Electricity created when conductor move through a magnetic field, cutting lines of flux and generating voltage and current. The key issue of wind energy conversion system is to feed power to grid with considering power quality issue means pure grid feeding so some advance type of power converter inverter topology has been implemented for pure grid feeding purpose.

DFIG based WECS is shown in figure 3.1. For variable speed wind turbine, the generator is controlled by power electronics equipment. The most common variable speed wind turbine generator is DFIG. A doubly fed induction generator is a standard, wound rotor induction machine with its stator is directly connected to the grid and its rotor winding is connected to the grid via back to back PWM converter- a machine side converter and grid side converter. The converter connected to the induction rotor circuit is the machine side converter and the converter connected to the grid side is grid side converter. These converters are working as inverter or rectifier depending on the condition of the DFIG.

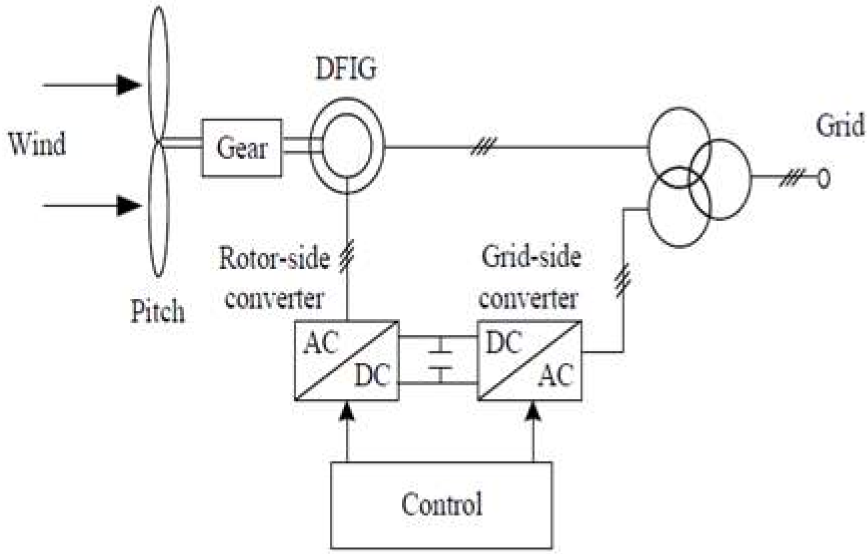

Figure 3.1: DFIG wind turbine configuration

Recently, design without the brushes have also been introduced. Alternatively, the rotor power could be magnetically transferred using the brushless doubly fed induction generator, which avoids the use of slip-rings. However, presently BDIGs are larger and more expensive than the slip-ring option and hence not common.

Since the back to back converter can operate in bi-directional mode. Here the speed range of DFIG is around 30% of synchronous speed. The maximum slip determines the maximum power to be processed by the rotor circuit, which is around 30% of the rated power. Therefore, the power flow in the rotor circuit is bidirectional: it can flow from the grid to the rotor or vice versa. When the DFIG is rotate at the speed less than synchronous speed the source to load means motoring action will take place and, in super-synchronous speed power is flow from load to source means generating action will take place. When the power flow is in the reverse direction, the grid side converter will act as a converter and the rotor-side converter will acts as inverter.

$$\omega_r < \omega_e \text{ sub-synchronous mode}$$
$$\omega_r > \omega_e \text{ super-synchronous mode}$$

The stator side always feed active power to the grid, whereas active power is fed into or out of the rotor is depending upon the operating condition of DFIG. In super-synchronous mode, active power flows from rotor via back to back converter to the grid whereas, it flows in opposite direction in sub-synchronous mode.

3.1.1 Features of DFIG

- The PMSG requires a power converter with full power processing capability, whereas a DFIG requires a smaller power converter to process the slip power. Thus smaller range of operating slip, smaller the required power converter. The size of power converter may affect the cost of energy.
- It has ability to control reactive power and to decoupled active and reactive power control by independently controlling the rotor excitation current.
- The DFIG has not necessarily to be magnetized from the power grid; it can be magnetized from the rotor circuit, too. It is also capable of generating reactive power that can be delivered to the stator by the grid-side converter. However, the grid-side converter normally operates at unity power factor and is not involved in the reactive power exchange between the turbine and the grid.
- DFIG system is capable of operating in four quadrants.

3.2 Mathematical Modeling of DFIG

In this section the basic mathematical modeling of DFIG is explained in detail with the consideration of the three-phase parameter transformed into two-phase parameter. Figure 3.2 shows the DFIG phase circuit. The stator and rotor phase winding are symmetrically distributed. The DFIG provides with laminated stator and rotor cores with uniform slots in which three-phase windings are placed. Usually, the rotor winding is connected to the copper slip-rings.

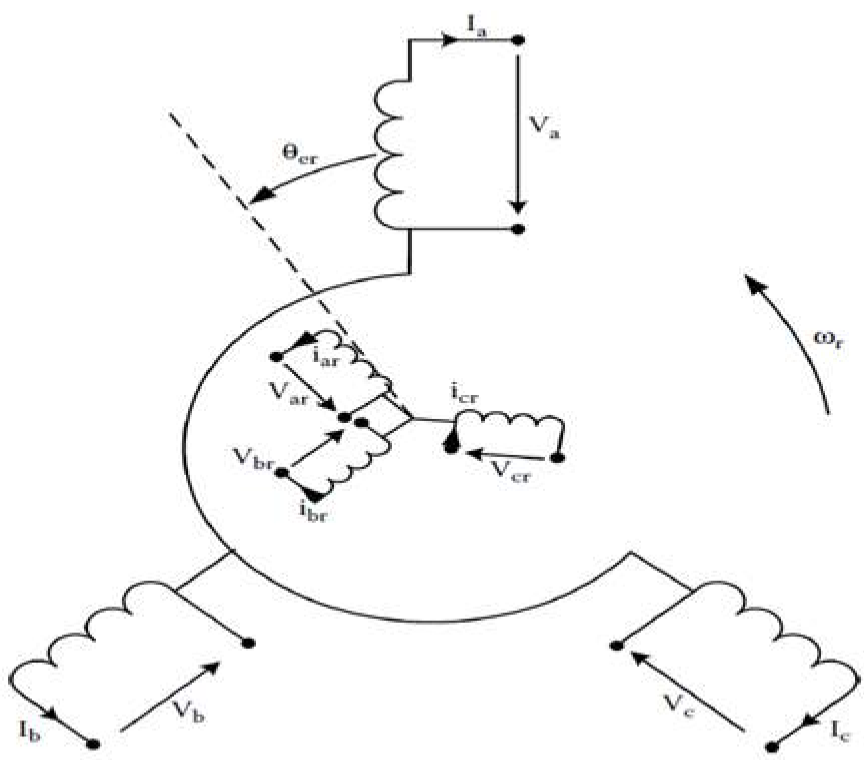

Figure 3.2: Doubly fed induction generator phase circuit

The voltage equations of stator and rotor in machine variables are,

$$I_a R_s + V_a = -\frac{d\psi_a}{dt} \tag{3.1}$$

$$I_b R_s + V_b = -\frac{d\psi_b}{dt} \quad (3.2)$$

$$I_c R_s + V_c = -\frac{d\psi_c}{dt} \quad (3.3)$$

$$I_{ar} R_r + V_{ar} = -\frac{d\psi_{ar}}{dt} \quad (3.4)$$

$$I_{br} R_r + V_{br} = -\frac{d\psi_{br}}{dt} \quad (3.5)$$

$$I_{cr} R_r + V_{cr} = -\frac{d\psi_{cr}}{dt} \quad (3.6)$$

The stator equations are written in stator coordinates, and the rotor equations are written in rotor coordinates, which explains the absence of motion-induced voltages. Generator mode association of voltage signs for both stator and rotor is evident. So, delivered electrical power are positive.

Stator variable are transformed into synchronously rotating (d-q) frame are;

$$V_{qs} = R_s I_{qs} + \frac{d\psi_{qs}}{dt} + \omega_e \psi_{ds} \quad (3.7)$$

$$V_{ds} = R_s I_{ds} + \frac{d\psi_{ds}}{dt} - \omega_e \psi_{qs} \quad (3.8)$$

The last terms are defined as the back emf of speed emf of counter emf. When angular speed ω_e is zero the speed emf due to d and q axis is zero and the equations changes to stationary form.

Owing to rotor circuit if the rotor is blocked or not moving i.e. ω_r=0, the machine equation can be written in similar way as stator equations.

$$V_{qr} = R_r I_{qr} + \frac{d\psi_{qr}}{dt} + \omega_e \psi_{dr} \quad (3.9)$$

$$V_{dr} = R_r I_{dr} + \frac{d\psi_{dr}}{dt} - \omega_e \psi_{qr} \quad (3.10)$$

Where, all parameter are referred to primary circuit, which is stator in this case. Let the rotor rotates at angular speed ω_r. Then the d-q axis fixed on the rotor fictitiously will move at relative speed ω_e-ω_r to the synchronously rotating frame.

The d-q frame rotor equations can be written by replacing ω_e-ω_r in place of ω_e as follows:

$$V_{dr} = R_r I_{dr} + \frac{d\psi_{dr}}{dt} + (\omega_e - \omega_r)\psi_{qr} \tag{3.11}$$

$$V_{dr} = R_r I_{dr} + \frac{d\psi_{dr}}{dt} - (\omega_e - \omega_r)\psi_{qr} \tag{3.12}$$

The flux linkage equations can be written as:

$$\psi_{qs} = L_{ls} I_{qs} + L_m(I_{qs} + I_{qr}) = L_s I_{qs} + L_m I_{qr} \tag{3.13}$$

$$\psi_{ds} = L_{ls} I_{ds} + L_m(I_{ds} + I_{dr}) = L_s I_{ds} + L_m I_{dr} \tag{3.14}$$

$$\psi_{qr} = L_{lr} I_{qr} + L_m(I_{qr} + I_{qs}) = L_r I_{qr} + L_m I_{qs} \tag{3.15}$$

$$\psi_{dr} = L_{lr} I_{dr} + L_m(I_{dr} + I_{ds}) = L_r I_{dr} + L_m I_{ds} \tag{3.16}$$

And,

$$\psi_{qm} = L_m(I_{qs} + I_{qr}) \tag{3.17}$$

$$\psi_{dm} = L_m(I_{ds} + I_{dr}) \tag{3.18}$$

Above equations describes the complete electrical modeling of DFIG. The equivalent circuit of DFIG in q-axis and d-axis is shown in figure 3.3 and 3.4 respectively. In this the machine is represented as two phase machine.

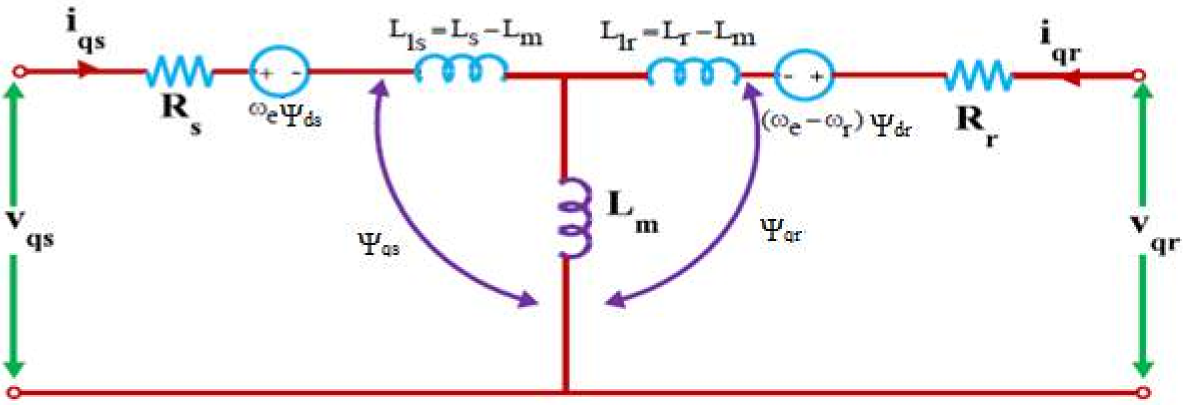

Figure 3.3: Space-phasor equivalent circuit of DFIG (q-axis circuit)

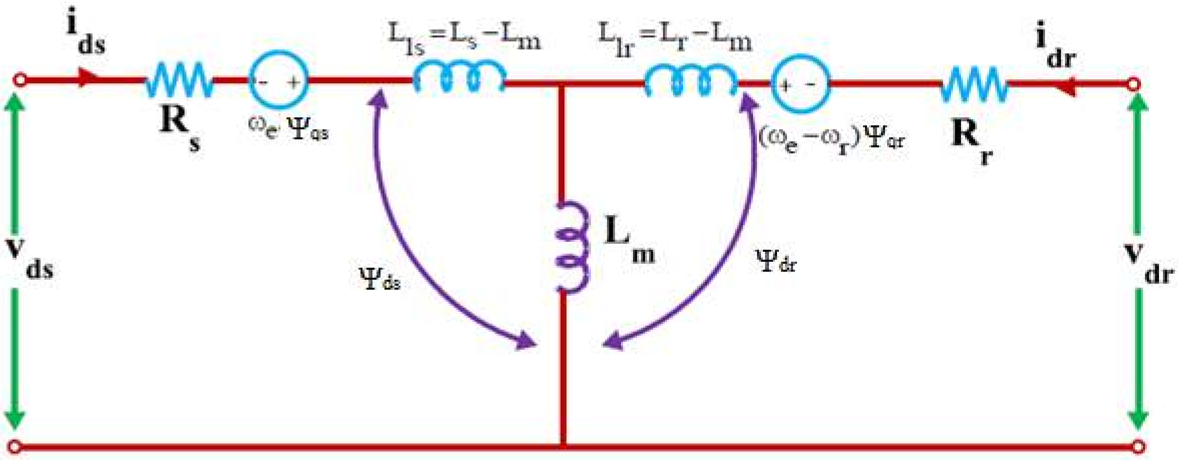

Figure 3.4: Space-phasor equivalent circuit of DFIG (d-axis circuit)

3.3 Power Electronics Converter

Nowadays the Back-to-Back converter is widely used in wind turbine applications. The back-to-back converter is composed by two identical Voltage Source Converters(VSC) and a capacitor which is connected in between them. The Figure 3.5 shows the B2B converter layout. power flow can be bidirectional, either it can go to the generator or to the grid. Therefore the VSC can work as a rectifier or as an inverter. At first step the AC is converted to DC through the generator side converter. Next, the DC is converted to AC through the grid side converter. Therefore in this case the generator side converter works as a rectifier and the grid side converter works as an inverter. The DC-link voltage must be higher than the peak main voltage and it is regulated by controlling the power flow to the AC grid. In fact one important property of the back-to-back converter is the possibility of fast control of the power flow.

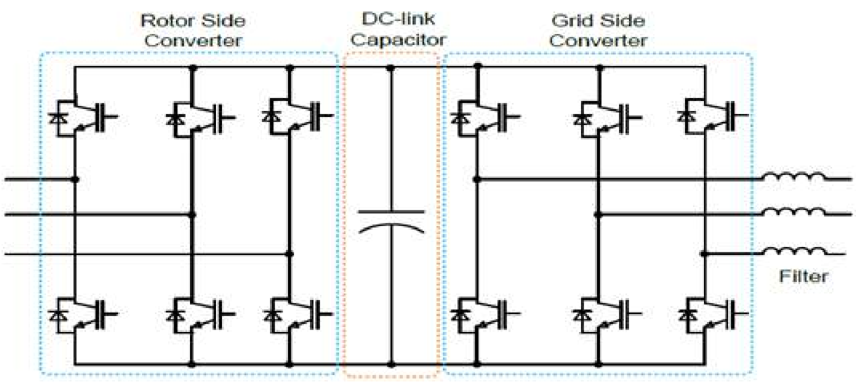

Figure 3.5: The AC/DC/AC bi-directional power converter in DFIG

With the generator side converter it is possible to control the torque and the speed of the generator, while the grid side converter keeps the DC-link voltage constant and unity power factor at grid side. The capacitor acts as filter for the voltage variations or ripple produced by the VSCs. Basically the Generator side converter controls the

Active and reactive power and and the Grid side converter maintains DC-link constant and unity power factor.

In normal operation, the RSC controls the speed and torque of generator and hence active and reactive power on the grid. Active power requirement for the RSC are provided by drawing current from or supplying current to the DC-link capacitor. GSC maintain the DC link voltage at set value regardless of the magnitude and the direction of the rotor power to guarantee a converter operation with unity power factor. The GSC can also to be used to enhance grid power quality. Each of these two PWM converter is control by using decoupled d-q control approaches.

3.3.1 Converter Model

The topology of a voltage source converter is the one presented in Figure3.6. The generator winding are star connected. Generator is connected to VSC.

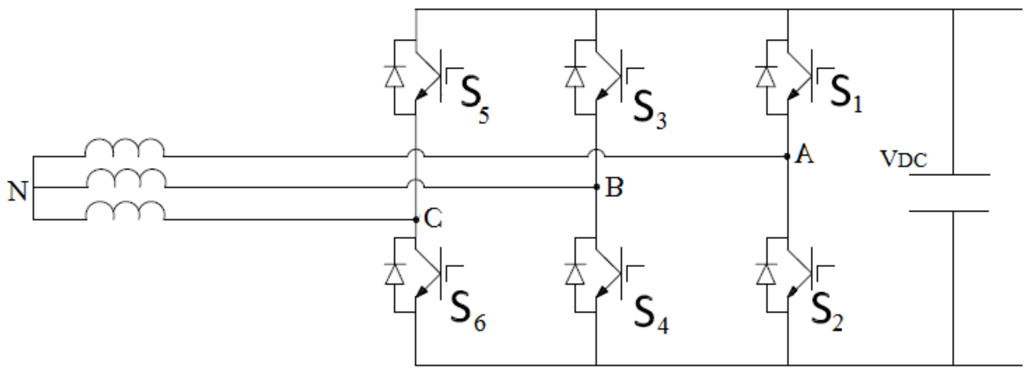

Figure 3.6: VSC with IGBT switches

As it can be seen in the Figure 3.6, a three phase converter has 6 semiconductors (IGBTs) displayed in three legs: A,B and C. The 6 semiconductors are considered as ideal switches. Only one switch on the same leg can be conducting at the same time. The line to line voltages is expressed as in the following equations:

$$V_{AB} = V_{AN} - V_{BN} \tag{3.19}$$

$$V_{BC} = V_{BN} - V_{CN} \tag{3.20}$$

$$V_{CA} = V_{CN} - V_{AN} \tag{3.21}$$

Where N is the negative DC bus and V_{AN}; V_{BN}; V_{CN} are the line to neutral voltage. Using kirchhof law it is known that in a three phase, three wire system the voltage (current) are equal zero.

$$V_{AN} + V_{BN} + V_{CN} = 0 \tag{3.22}$$

The two equations 3.19, 3.20, 3.21 and 3.22, can be rearrange in such a way that a new formula for the phase voltage can be formulated:

$$\begin{pmatrix} V_{AN} \\ V_{BN} \\ V_{CN} \end{pmatrix} = \frac{1}{3} \begin{pmatrix} 1 & 0 & -1 \\ -1 & 1 & 0 \\ 0 & -1 & 1 \end{pmatrix} \begin{pmatrix} V_{AB} \\ V_{BC} \\ V_{CA} \end{pmatrix} \tag{3.23}$$

The switching states of each leg are representing by three variables: D_a, D_b, D_c named duty cycles. This variables can have just two values "1" when the switch is turn on and "0" when switch is turn off. The switching states together with the DC voltage ca give expression for the line to line voltages of the converter:

$$\begin{pmatrix} V_{AB} \\ V_{BC} \\ V_{CA} \end{pmatrix} = V_{DC} \begin{pmatrix} 1 & 0 & -1 \\ -1 & 1 & 0 \\ 0 & -1 & 1 \end{pmatrix} \begin{pmatrix} D_a \\ D_b \\ D_c \end{pmatrix} \tag{3.24}$$

After a few simplification in the equations 3.23 and 3.24 the phase voltage is expressed with the help of DC voltage and switching state as presented in equation 3.25:

$$\begin{pmatrix} V_{AN} \\ V_{BN} \\ V_{CN} \end{pmatrix} = \frac{V_{DC}}{3} \begin{pmatrix} 2 & -1 & -1 \\ -1 & 2 & -1 \\ -1 & -1 & 2 \end{pmatrix} \begin{pmatrix} D_a \\ D_b \\ D_c \end{pmatrix} \tag{3.25}$$

Having the duty cycles and the phase currents, the DC current can be deduct as in the following:

$$I_{DC} = \begin{pmatrix} D_a & D_b & D_c \end{pmatrix} \begin{pmatrix} I_A \\ I_B \\ I_c \end{pmatrix} \tag{3.26}$$

3.4 Control strategies of DFIG

The DFIG-based WECS control system consists of two parts: the electrical control of the DFIG and the mechanical control of the wind turbine speed and blade pitch angle. Control of the DFIG is achieved by control of the variable frequency converter, which includes control of the RSC and control of the GSC. By controlling the converters on both sides, the DFIG characteristics can be adjusted so as to achieve maximum of effective power conversion or capturing capability for a wind turbine and to control its power generation with less fluctuations. However to meet these needs, the grid side converter should be controlled in such a way to maintain a constant DC link capacitor voltage and to keep the converter operation at desired power factor. The objective of the RSC is to allow the DFIG wind turbine for decoupled control of active and reactive power.

Realization of vector control principle for decoupling of generators active and reactive power , improvement of overall power factor, less distortion in currents are the functional characteristics of the back to back converters.

3.4.1 Vector control of RSC

The wound rotor induction generator is controlled using a synchronously rotating reference frame, with the quadrature axis oriented along the stator flux vector position and the direct axis oriented along the active power. In this manner, a decoupled control between the stator side active and reactive power can be achieved.

Under the stator flux control scheme, all the stator and rotor variables are needed to be converted to the synchronously rotating stator flux reference frame. The space vector diagram which shows the relationship between the stator flux reference frame and the stationary reference frame is shown in Figure.

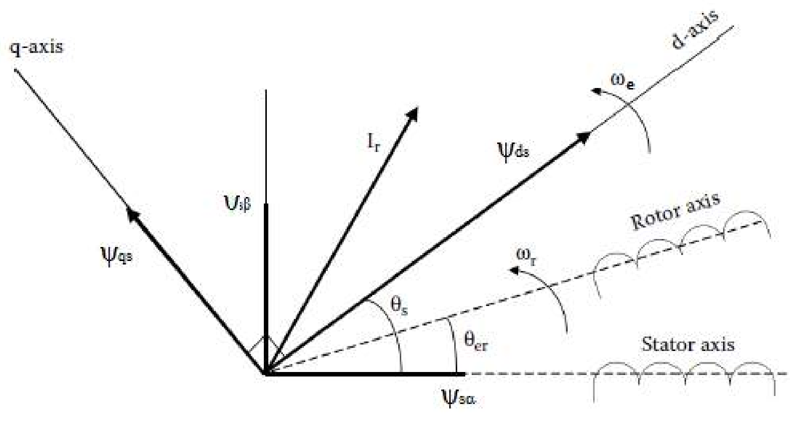

Figure 3.7: Location of different vector in stationary coordinates

Where, $\psi_{s\alpha}$ and $\psi_{s\beta}$, are the stator flux linkages expressed in the stationary α, β reference frame. The stator flux angular position, θ_s can be obtained by following equation:

$$\theta_s = \tan^{-1} \frac{\psi_{s\beta}}{\psi_{s\alpha}} \tag{3.27}$$

Where,

$$\psi_{s\alpha} = L_s I_{s\alpha} + L_m I_{r\alpha} \tag{3.28}$$

$$\psi_{s\beta} = L_s I_{s\beta} + L_m I_{r\beta} \tag{3.29}$$

Where, $I_{s\alpha}$, $I_{s\beta}$ are stator -axis and -axis current and $I_{r\alpha}$, $I_{r\beta}$ are rotor α-axis and β-axis currents expressed in stationary reference frame. We can obtain it by using Clarke transformation.

After obtaining the stator angular position θ_s all the stator and rotor variables of the DFIG can be transformed to the stator flux reference frame.

$$\psi_{ds} = |\psi_s| = \sqrt{{\psi_{s\alpha}}^2 + {\psi_{s\beta}}^2} \tag{3.30}$$

$$\psi_{qs} = 0 \tag{3.31}$$

ψ_{ds} is d-axis stator flux linkage and ψ_{qs} is q-axis stator flux linkage.

$|\psi_s|$ is magnitude of stator flux linkage.

Since the stator of DFIG is directly connected to the grid, and the influence of the stator resistance is small, the d-axis stator flux linkage can be considered as constant and q-axis stator flux linkage can be treated as zero.

So,

$$|\psi_s| = L_m I_{ms} = \psi_{ds} = L_s I_{ds} + L_m I_{dr} \tag{3.32}$$

Hence,

$$I_{ds} = \frac{(L_m I_{ms} - L_m I_{dr})}{L_s} \tag{3.33}$$

$$\psi_{qs} = 0 = L_s I_{qs} + L_m I_{qr} \tag{3.34}$$

Hence,

$$I_{qs} = -\frac{L_m I_{qr}}{L_s} \tag{3.35}$$

And,

$$\psi_{dr} = L_r I_{dr} + L_m I_{ds} = \frac{L_m^2}{L_s} I_{ms} + \sigma L_r I_{dr} \tag{3.36}$$

$$\psi_{qr} = L_r I_{qr} + L_m I_{qs} = \sigma L_r I_{qr} \tag{3.37}$$

$$V_{dr} = R_r I_{dr} + \frac{d\psi_{dr}}{dt} - (\omega_s - \omega_r)\psi_{qr} \tag{3.38}$$

$$V_{dr} = R_r I_{dr} + \sigma L_r \frac{dI_{dr}}{dt} - (\omega_s - \omega_r) L_r I_{qr} \tag{3.39}$$

$$V_{qr} = R_r I_{qr} + \frac{d\psi_{qr}}{dt} + (\omega_s - \omega_r)\psi_{dr} \tag{3.40}$$

$$V_{qr} = R_r I_{qr} + \sigma L_r \frac{dI_{qr}}{dt} + (\omega_s - \omega_r)(\frac{L_m^2}{L_s} I_{ms} + \sigma L_r I_{dr}) \tag{3.41}$$

Where,

$$\sigma = 1 - \frac{L_m^2}{L_s L_r} \tag{3.42}$$

Here, ψ_{dr} and ψ_{qr} are the d-q axes rotor flux linkages, I_{ds} and I_{qs} are d-q axes stator current, while I_{dr} and I_{qr} are d-q axes rotor current I_{ms} is magnetizing current of DFIG, while V_{dr} and V_{qr} are d-q axes rotor terminal ω_s is electrical angular velocity of stator flux which is equal to synchronous speed.

Equation 3.40 and 3.41 constitute DFIG model expressed in the stator flux reference frame. In which the stator voltage equations in the DFIG fourth order model are eliminated due to the fact that under this reference frame, the direct axis stator terminal voltage will be equal to zero and quadrature-axis stator terminal voltage to be constant.

The stator d-q axis terminal voltage expression as well as the relationship between torque, power and the d-q axes stator current, rotor currents expressed in the stator flux reference frame can be deduced as follow.

$$|\psi_s| = |\psi_{ds}| = constant \tag{3.43}$$

$$\psi_{qs} = 0 \tag{3.44}$$

$$V_{ds} = R_s I_{ds} + \frac{d\psi_{ds}}{dt} - \omega_s \psi_{qs} \tag{3.45}$$

$$V_{qs} = R_s I_{qs} + \frac{d\psi_{qs}}{dt} + \omega_s \psi_{ds} = constant \tag{3.46}$$

Hence,

$$V_{ds} = 0 \tag{3.47}$$

$$|V_{qs}| = |V_s| = constant \tag{3.48}$$

Accordingly develop Torque, Active and Reactive powers are,

$$T_{dev} = \frac{3}{2}\frac{p}{2}[\psi_{ds} I_{qs} - \psi_{qs} I_{ds}] \tag{3.49}$$

$$T_{dev} = \frac{3}{2}\frac{p}{2}\psi_{ds} I_{qs} = \frac{3}{2}\frac{p}{2}\frac{L_m^2}{L_s} I_{ms} I_{qr} \tag{3.50}$$

$$P_s = \frac{3}{2}(V_{ds} I_{ds} + V_{qs} I_{qs}) = \frac{3}{2} V_{qs} I_{qr} \tag{3.51}$$

$$P_s = \frac{3}{2}|V_s|\frac{L_m}{L_s} I_{qr} \tag{3.52}$$

$$Q_s = \frac{3}{2}(V_{qs} I_{ds} - V_{ds} I_{qs}) = \frac{3}{2} V_{qs} I_{ds} \tag{3.53}$$

$$Q_s = \frac{3}{2}|V_s|\frac{L_m}{L_s}(I_{ms} - I_{dr}) \tag{3.54}$$

From the equations 3.40 and 3.41, it can be seen that the stator terminal voltage equations are eliminated, which means that the DFIG fourth order model is reduced to a second order model expressed in the stator flux reference frame. Due to the constant stator voltages, the stator active power and reactive power can be controlled in a decoupled manner via the stator currents I_{qs} and I_{ds} and further via rotor current I_{qr} and I_{rs} respectively. This is because the stator current can be directly regulated by rotor current as shown in equations 3.33 and 3.35.

The angular position of the supply voltage θ_e is calculated:

$$\theta_e = \tan^{-1}\frac{V_{g\beta}}{V_{g\alpha}} \tag{3.55}$$

The rotor electrical position θ_{er}:

$$\theta_{er} = p_1\theta_r; p_1 = polepair. \tag{3.56}$$

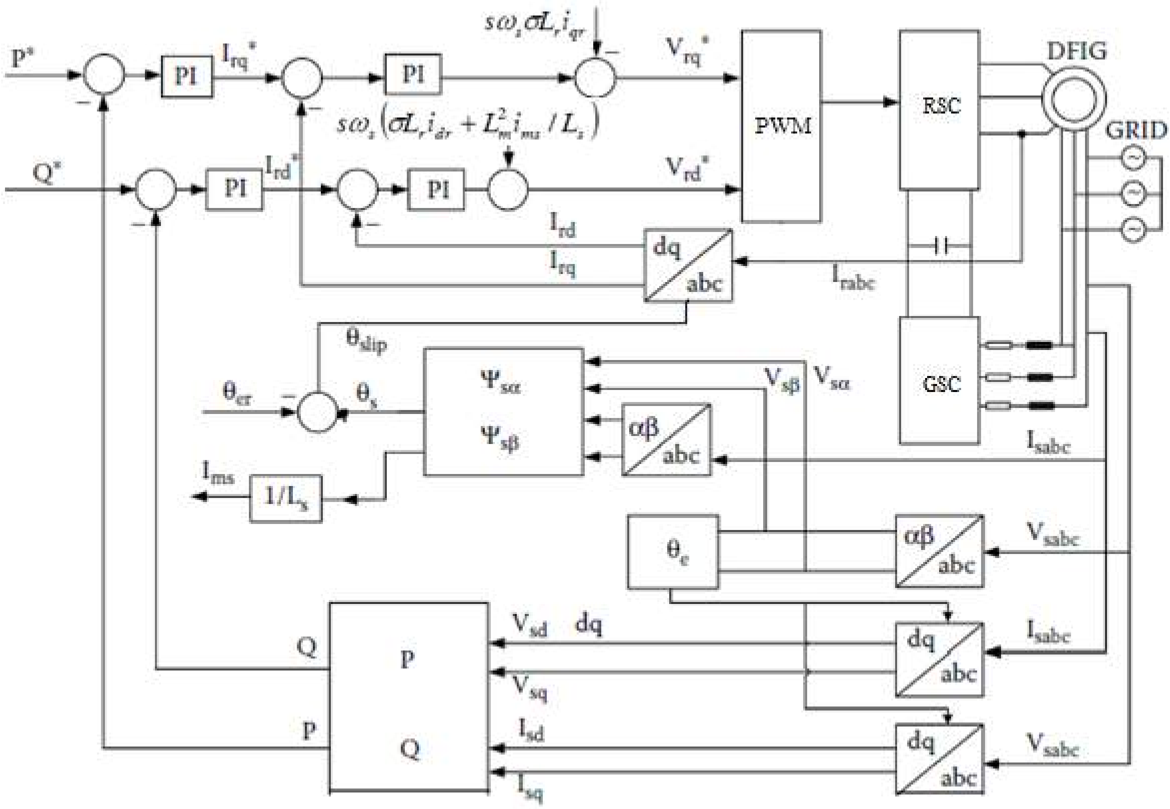

Figure 3.8: Vector control principle of the machine-side converter

Figure 3.8 shows the vector control scheme for the generator-side PWM voltage source converter. The control scheme utilizes a cascade control, i.e. the inner current control loops are used for controlling the d- and q-axes rotor currents, and the outer power control loops are used to control the active and reactive power at the stator terminals. The reference active and reactive power are compared with actual power and the error is processed through PI controller. It will generates the reference value of rotor current I_{qr} and I_{dr} respectively, Then it compared with the actual rotor current, error is processed through PI controller. The output of PI controllers, V_{dr} and V_{qr} are the dq-axis rotor voltage references in the synchronous frame, which are transformed into a three-phase reference for rotor voltages, V_{ar}, V_{br} and V_{cr} in the stationary frame. The rotor reference voltages can serve as the three-phase modulating signal and they are compared with the triangle waveform and it will generates the gate pulses for the switches of rotor side converter.

3.4.2 Vector control of GSC

The objective of the grid-side converter controller is to keep the DC-link voltage constant regardless of the magnitudes of the grid-side voltages, and to yield a unity power factor looking into the WECS from the grid-side. In order to acquire better control performances, a feed forward control is used to decouple the D- and Q axes components for the grid-side converter. Moreover, a vector control scheme, with a reference frame oriented along the grid voltage vector position, is used to independently control the active and reactive power flow between the grid and the grid-side converter.
Figure 3.9 shows the schematic diagram of source side voltage converter. The PWM converter is current regulated with the direct axis current is used to regulate the DC link voltage and the quadrature axis current component is used to regulate the reactive power. The reactive power demand set to zero to ensure unity power factor operation.

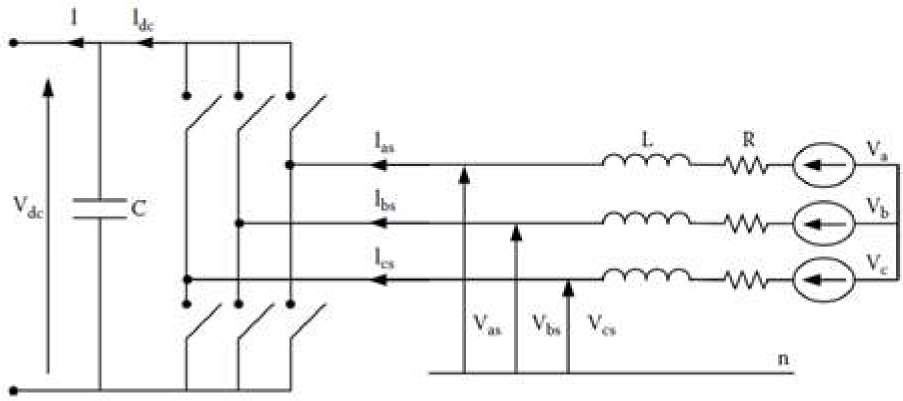

Figure 3.9: Source-side voltage converter.

The voltage equations across the inductor are as follows:

$$V_a = R_s I_{as} + L\frac{dI_{as}}{dt} + V_{as} \tag{3.57}$$

$$V_b = R_s I_{bs} + L\frac{dI_{bs}}{dt} + V_{bs} \tag{3.58}$$

$$V_c = R_s I_{cs} + L\frac{dI_{cs}}{dt} + V_{cs} \tag{3.59}$$

The equation may be translated into d-q synchronous coordinates that may be aligned to axis d voltage (V_q=0,V_d=V_s).

$$V_d = RI_{dg} + L\frac{dI_{dg}}{dt} - \omega_e LI_{qg} + V_{dg} \tag{3.60}$$

$$V_q = RI_{qg} + L\frac{dI_{qg}}{dt} + \omega_e LI_{dg} + V_{qg} \tag{3.61}$$

Where, ω_e is the speed of reference system or the supply frequency.
Where V_d and V_q are two phase voltages found from V_a, V_b and V_c using d-q theory.
Neglecting the harmonics due to switching in the converter and the machine losses and converter losses, the active power balance equation is as follows:

$$V_{dc}I_{dc} = \frac{3}{2}V_dI_d = P_r; V_q = 0 \tag{3.62}$$

And the Reactive power Q_r is,

$$Q_r = \frac{3}{2}(V_dI_q - V_qI_d) = \frac{3}{2}V_dI_q; V_q = 0 \tag{3.63}$$

Consequently, the reactive power from the power source to (from) the source-side converter may be controlled through I_q.

From the equation 3.63, the d-q axes component have coupling components ω_e LI_{qg} and ω_e LI_{dg} . therefore a voltage de-coupler scheme is recommended and corresponding control signal are,

$$V_{ds}^{'} = \omega_e LI_q + V_{dg} \tag{3.64}$$

$$V_{qs}^{'} = -\omega_e LI_d \tag{3.65}$$

Figure 3.10 shows the vector control scheme for grid side converter, The reference DC-link voltage and reactive power are compared with the actual quantity, the error is processed through the PI controller and it will generate the reference value of rotor currents. These currents are compared with actual currents and the the generated signal are converted into the three phase signal at the stator voltage angle. These signal are compared with triangle signal and it will generates the gate pulses for the switches of grid side converter.

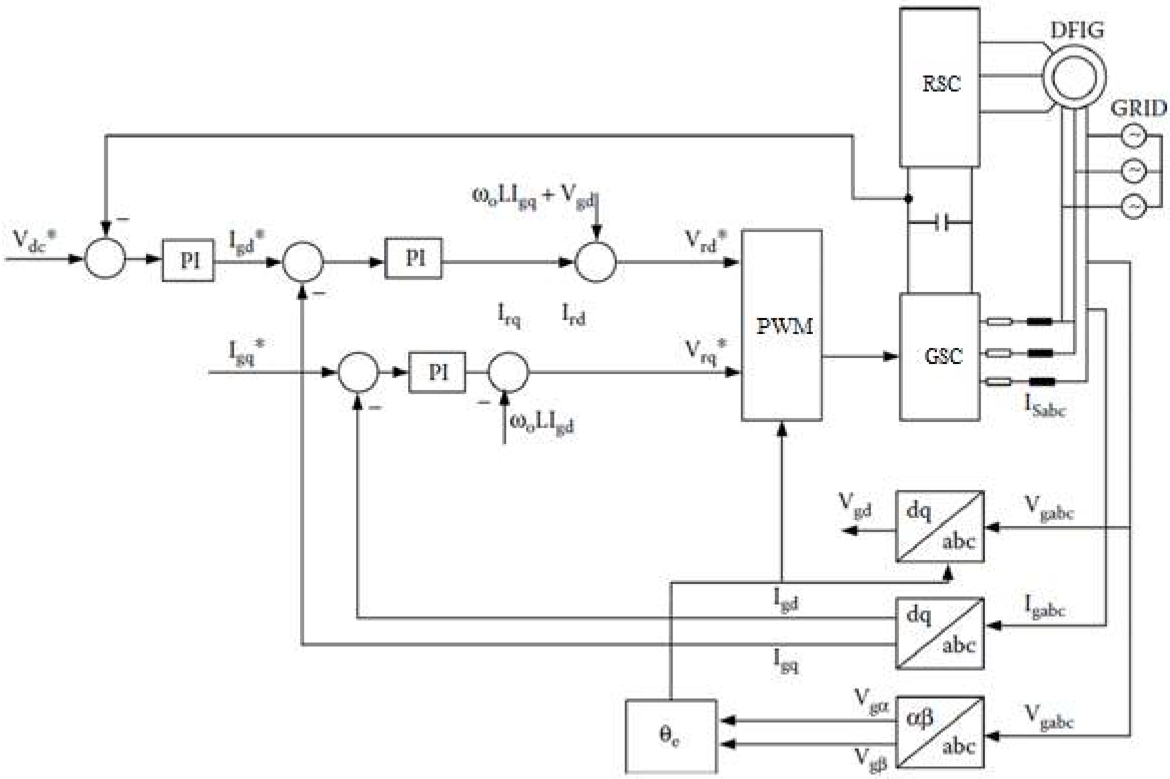

Figure 3.10: Vector control principle of Grid-Side converter

Chapter 4

SIMULATION RESULTS AND ANALYSIS

4.1 Wind turbine model

$$P_{out} = \frac{1}{2} \rho A V^3 C_p$$

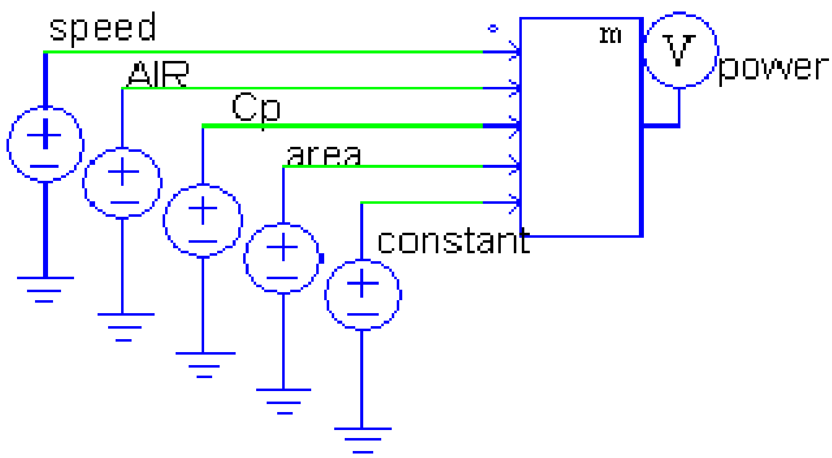

Figure 4.1: Wind turbine model

Figure 4.1 shows the wind turbine model based on the equation the turbine generates the 2 MW power. Here the power coefficient is assumed as 0.4916, the wind speed is 12.5 m/s and the Air density is 1.225 kg/m^3. As shown in Figure4.2 wind turbine generates 2MW power.

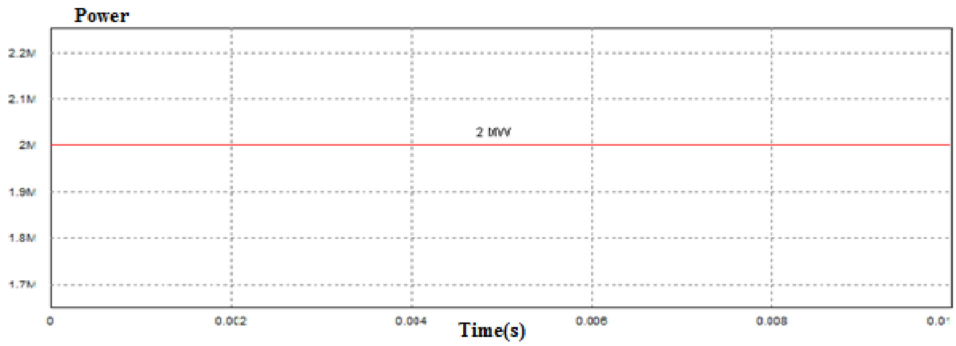

Figure 4.2: Output power

Scale: output power: X-axis: 1 Div=0.002 sec, Y-axis: 1 Div=0.1 MW.

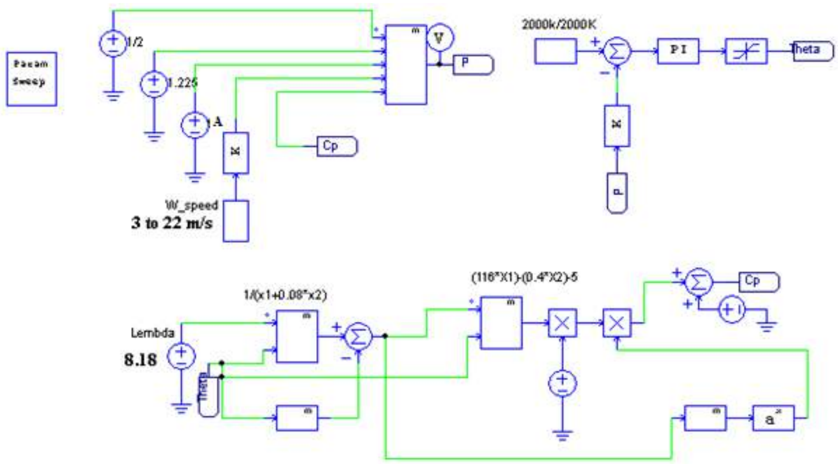

Figure 4.3: Aerodynamic model of wind turbine

Figure 4.3 shows the aerodynamic model of wind turbine. The speed is varying from 3 m/s to 23 m/s. from the output of the wind turbine model it shows that upto rated speed the power generating in MPPT mode and from the rated speed the generating power is controlled by controlling pitch angle of the blade. Here the optimum value of power coefficient is considering is 0.49 and the optimum value of the tip speed ratio is 8.18.

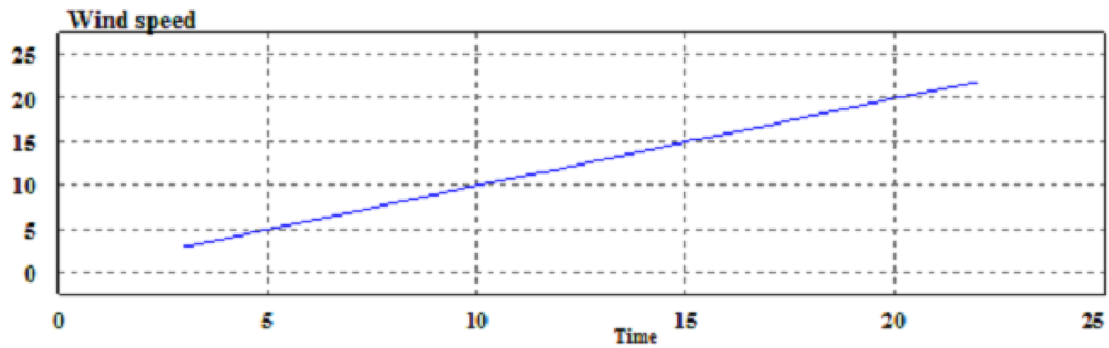

Figure 4.4: wind speed

Scale: wind speed: X-axis: 1 Div=5 sec, Y-axis: 1 Div=5 m/s.

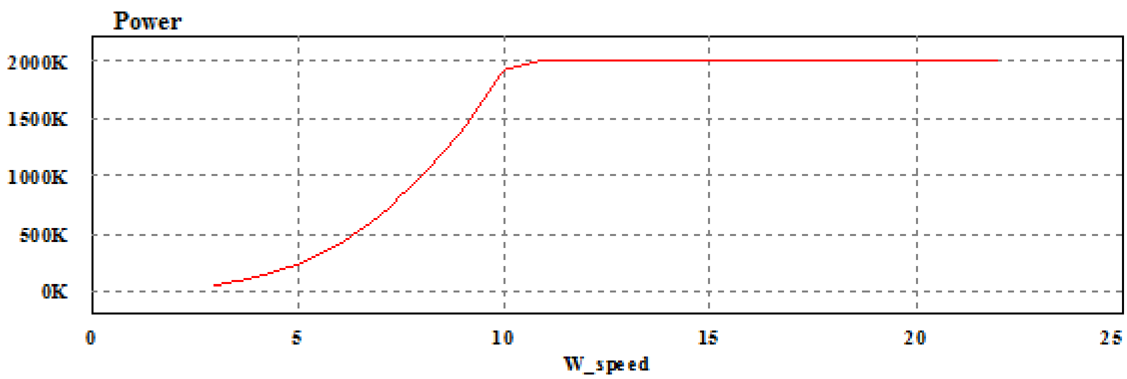

Figure 4.5: Output power at variable speed

Scale: output power: X-axis: 1 Div=5 sec, Y-axis: 1 Div=500 kVA

The maximum power (from equation 2.13) can be extract below the rated speed (3 m/s to 10 m/s) by keeping the value of C_p at 0.4916 using MPPT. Above rated speed the power is remaining 2 MW and it can be controlled by blade pitch angle control as shown in table I.

Table I: Wind Turbine Output Power with Pitch angle Control

Wind Speed	**Power (kW)**	**Pitch angle (degree)**	C_p
3	51.72	0	0.4916
4	122.6	0	0.4916
5	239.4	0	0.4916
6	413.7	0	0.4916
7	657.0	0	0.4916
8	980.8	0	0.4916
9	1396.5	0	0.4916
10	1915.6	0	0.4916
11	2000	3.67	0.3856
12	2000	8.70	0.2970
13	2000	11.70	0.2336
14	2000	13.69	0.1870
15	2000	15.09	0.1520
16	2000	16.12	0.1253
17	2000	16.89	0.1044
18	2000	17.49	0.0880
19	2000	17.96	0.0748
20	2000	18.33	0.0641
21	2000	18.64	0.0554
22	2000	18.88	0.0482
23	2000	19.09	0.0421

4.2 DFIG system

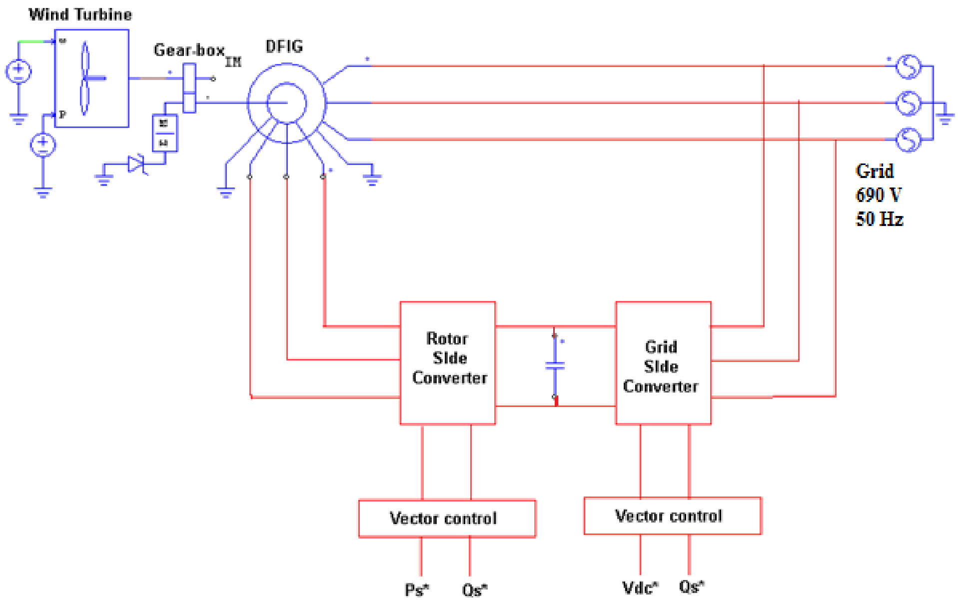

Figure 4.6: DFIG system

Figure 4.6 shows the simulation of DFIG system in PSIM software.

The 2MW, 690 V system is simulated, The wind turbine is connected to the DFIG through gear-box, which converts low speed to high speed, So DFIG is can rotate at super-synchronous speed. the stator of DFIG is directly connected to the grid and rotor is connected to the grid via back-to-back converter. The RSC controls the active and reactive power and GRC is control the dc-link voltage.

4.2.1 Rotor side converter control

Rotor side converter control has been simulated in PSIM as shown in Figure 4.7.

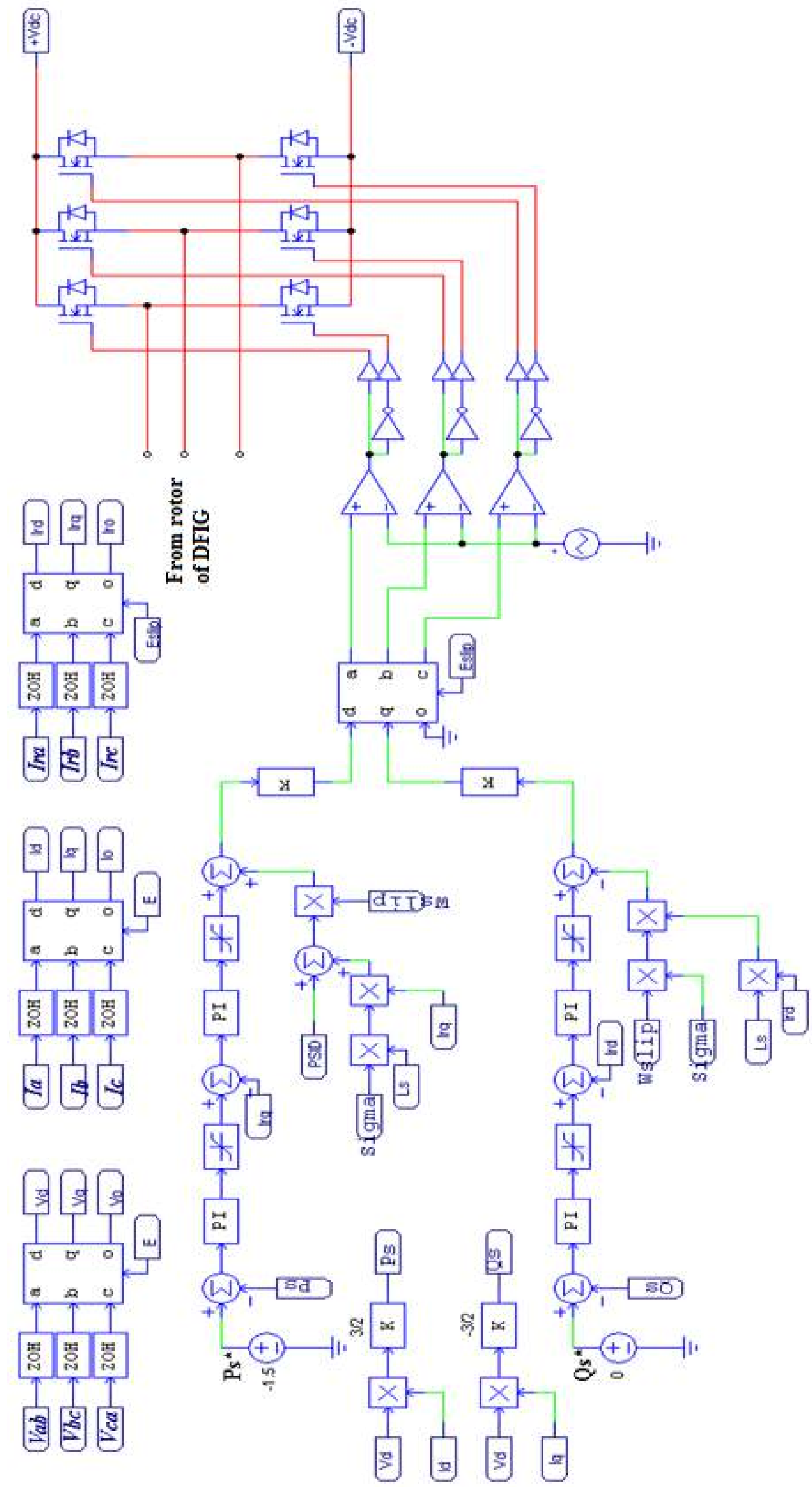

Figure 4.7: Control for rotor side converter

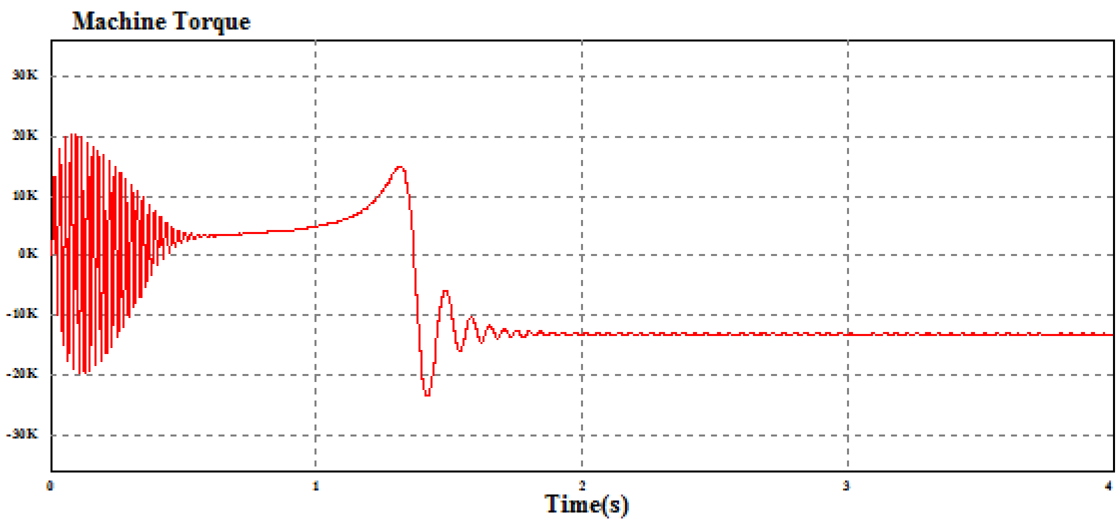

Figure 4.8: Machine Torque

Scale: Torque: X-axis: 1 Div=1 sec, Y-axis: 1 Div=10k Nm

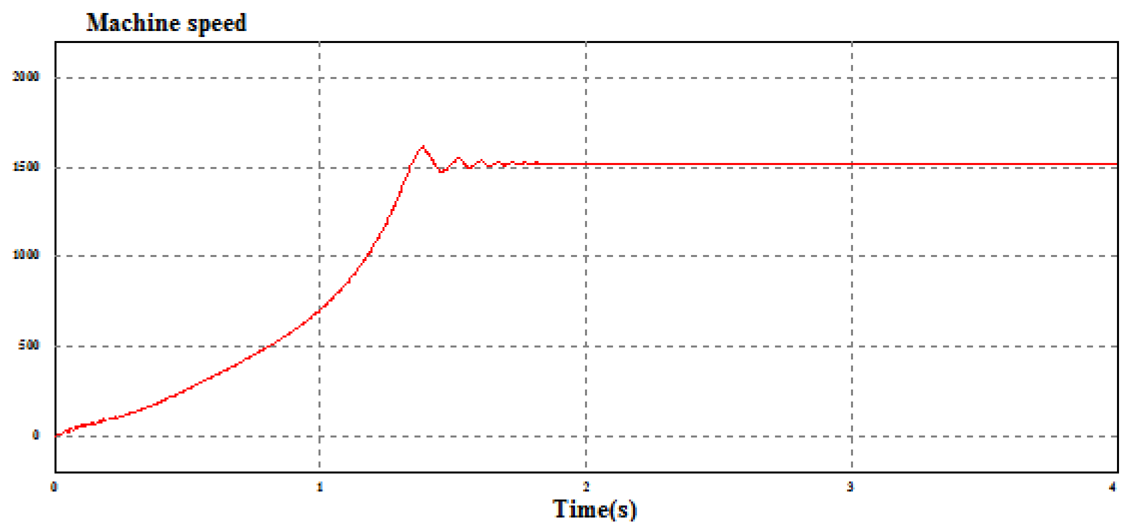

Figure 4.9: Machine speed

Scale: Speed: X-axis: 1 Div=1 sec, Y-axis: 1 Div=500 rpm

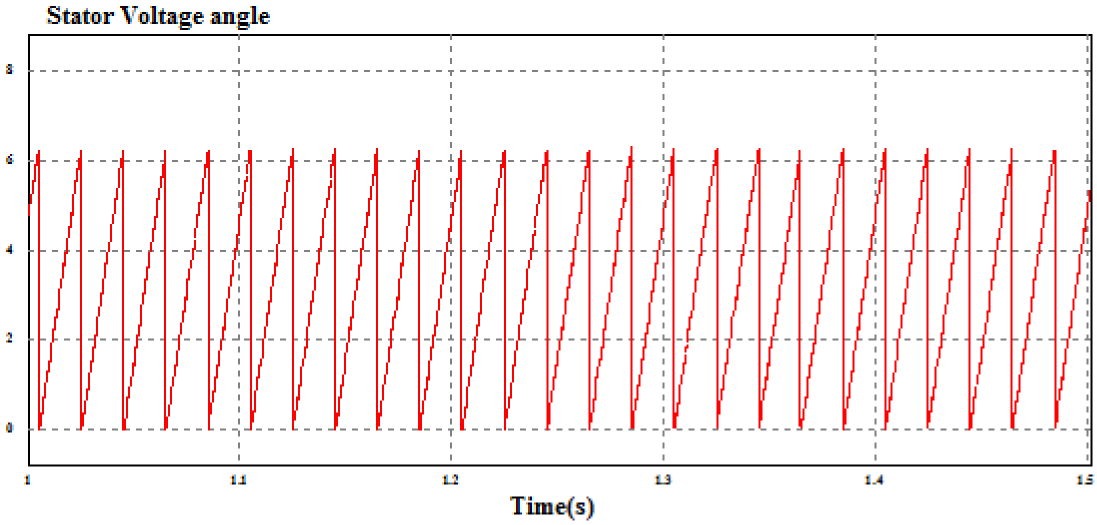

Figure 4.10: Stator voltage angle

Scale: Voltage: X-axis: 1 Div=0.1 sec, Y-axis: 1 Div=2.

Figure 4.8 shows machine torque which 13 kNm and Figure 4.9 shows the machine speed which is 1520 rpm, hence machine runs at super-synchronous speed and it will generates the electrical power. Figure 4.10 shows the stator voltage angle at which all the stator quantities are converted into the synchronously rotating reference frame.

Figure 4.12 shows the grid voltage 398.4 V rms (phase voltage) and Figure 4.14 shows the grid current 1677 Amp rms. THD in line current is follow:

A-phase : 4.95%

B-phase : 4.98%

C-phase : 4.96%

which is less than 5% according to IEEE 519 norms.

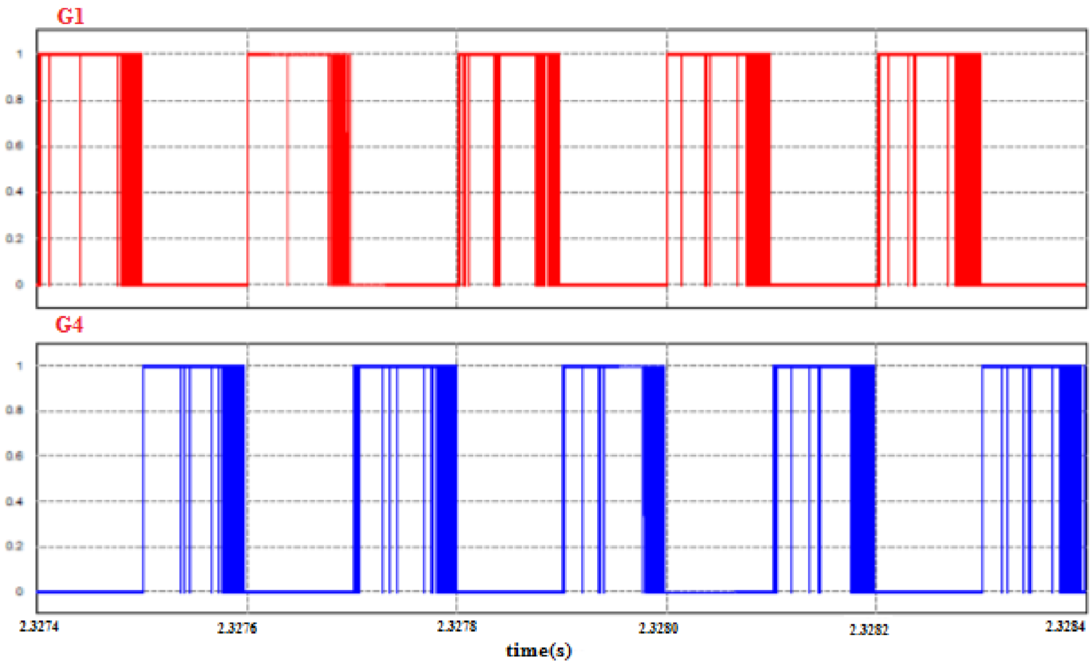

Figure 4.11: Gate pulses for Switch 1 and 4

Scale: Speed: X-axis: 1 Div=0.0002 sec, Y-axis: 1 Div=0.2

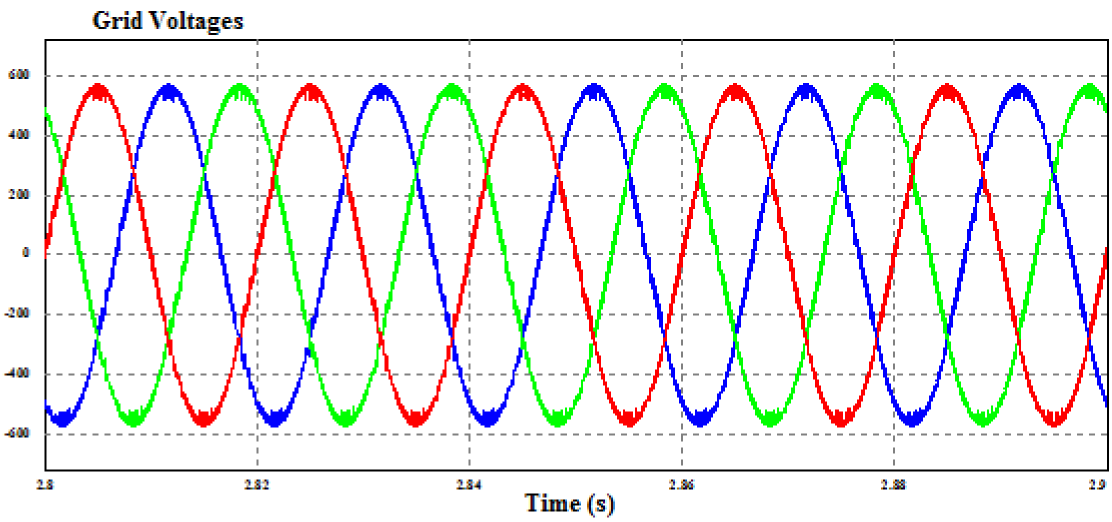

Figure 4.12: Grid Voltage

Scale: Voltage: X-axis: 1 Div=0.02 sec, Y-axis: 1 Div=200 V.

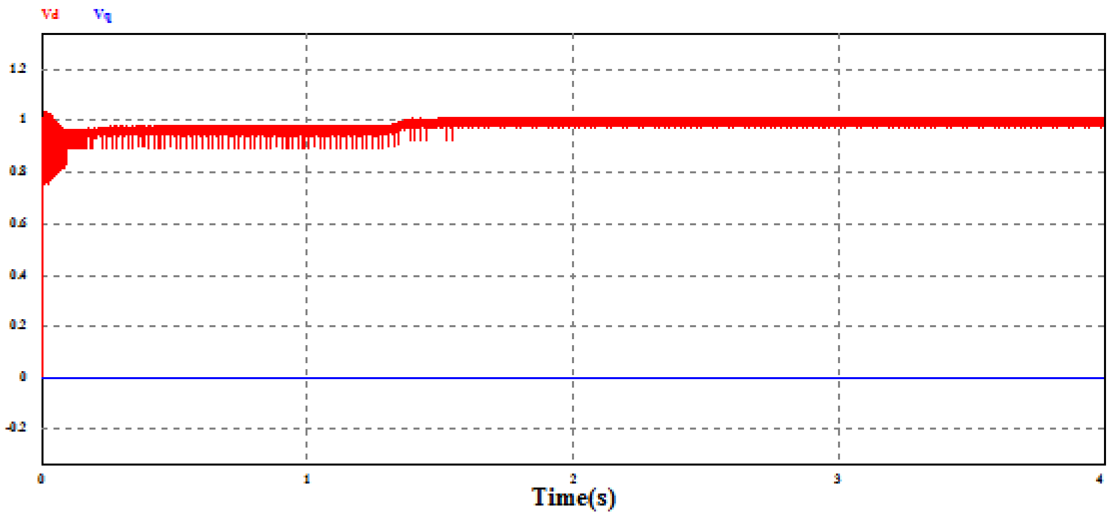

Figure 4.13: Stator voltage in d-q axes

Scale: Voltage: X-axis: 1 Div=1 sec, Y-axis: 1 Div=0.2 pu.

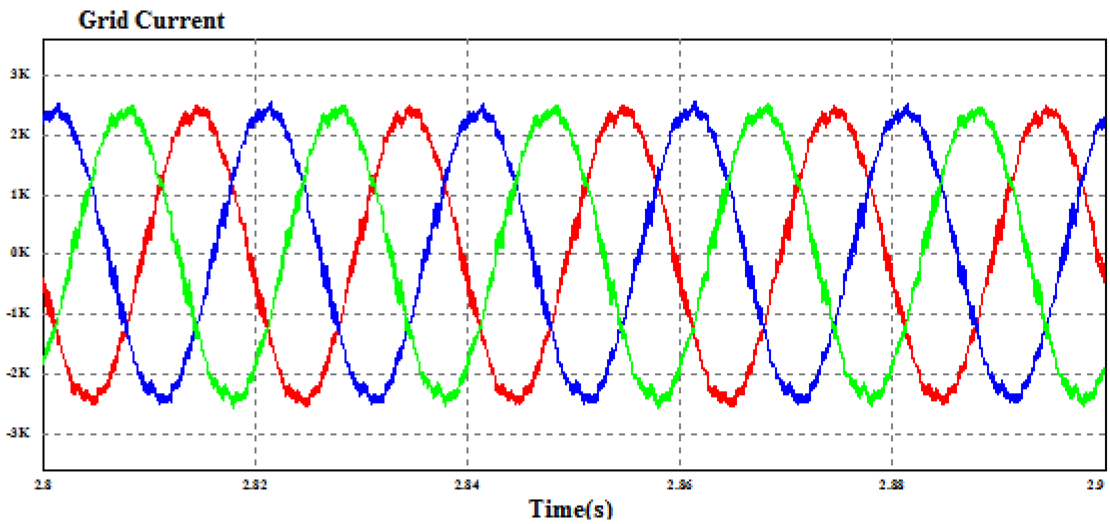

Figure 4.14: Grid current

Scale: Current: X-axis: 1 Div=0.02 sec, Y-axis: 1 Div=2k Amp.

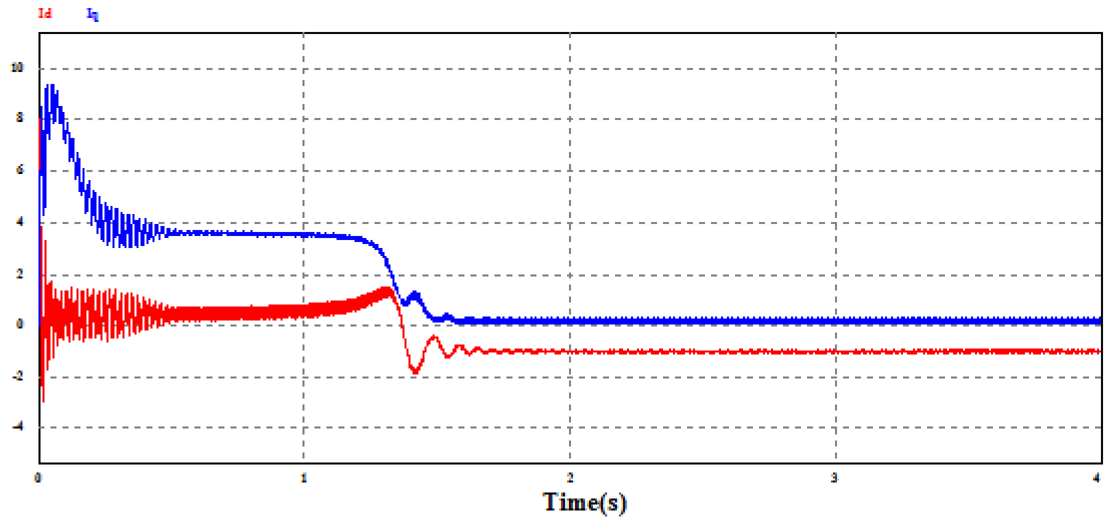

Figure 4.15: Stator current in d-q axes

Scale: d-axis current(Red): X-axis: 1 Div=1 sec, Y-axis: 1 Div=2 pu.
q-axis current (Blue): X-axis: 1 Div=1 sec, Y-axis: 1 Div=2 pu.

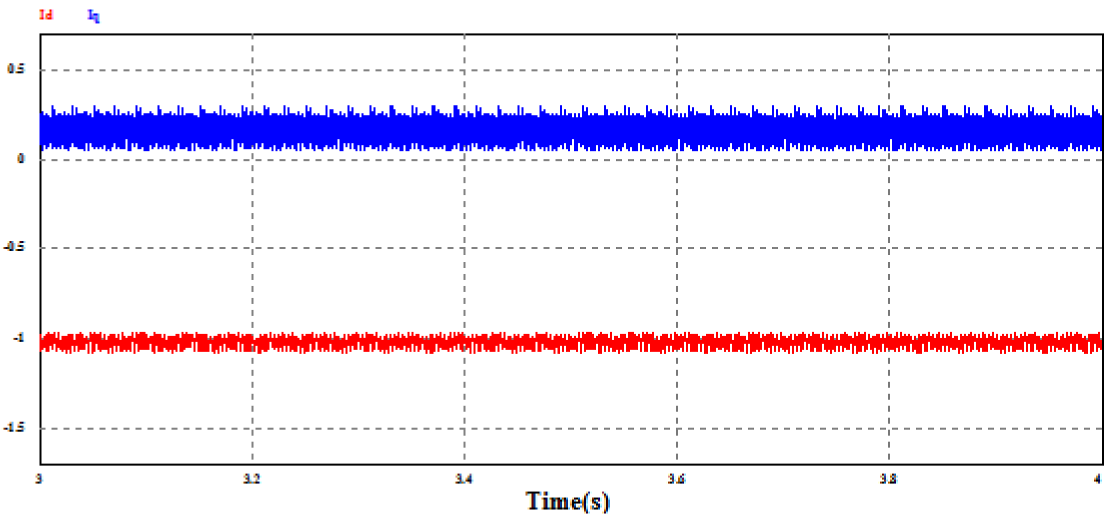

Figure 4.16: Stator current in d-q axes

Scale: d-axis current(Red): X-axis: 1 Div=0.2 sec, Y-axis: 1 Div=0.5 pu.
q-axis current (Blue): X-axis: 1 Div=0.2 sec, Y-axis: 1 Div=0.5 pu.

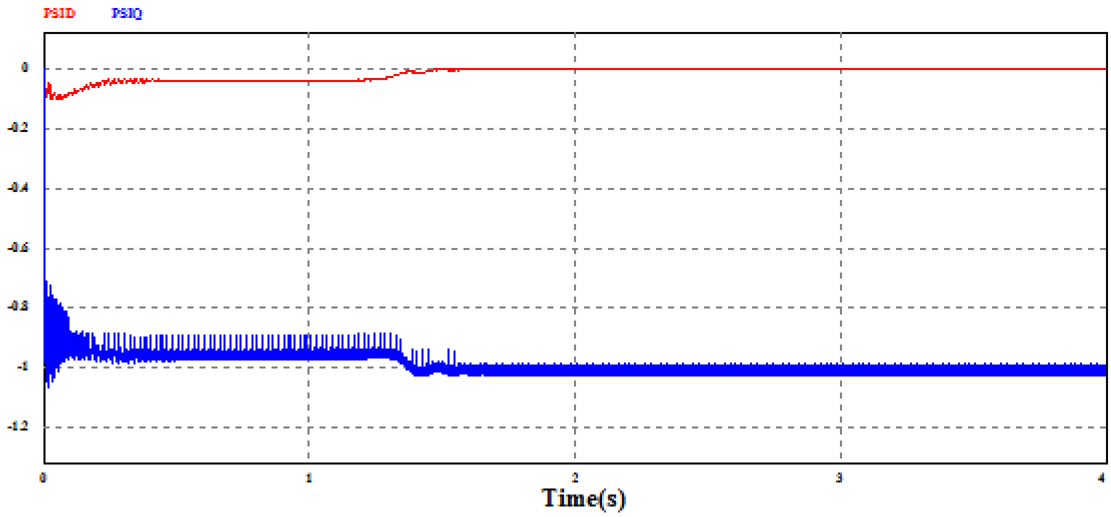

Figure 4.17: Stator flux in d-q axis

Scale: d-axis flux(Red): X-axis: 1 Div=1 sec, Y-axis: 1 Div=0.2 pu.
q-axis flux (Blue): X-axis: 1 Div=1 sec, Y-axis: 1 Div=0.2pu.

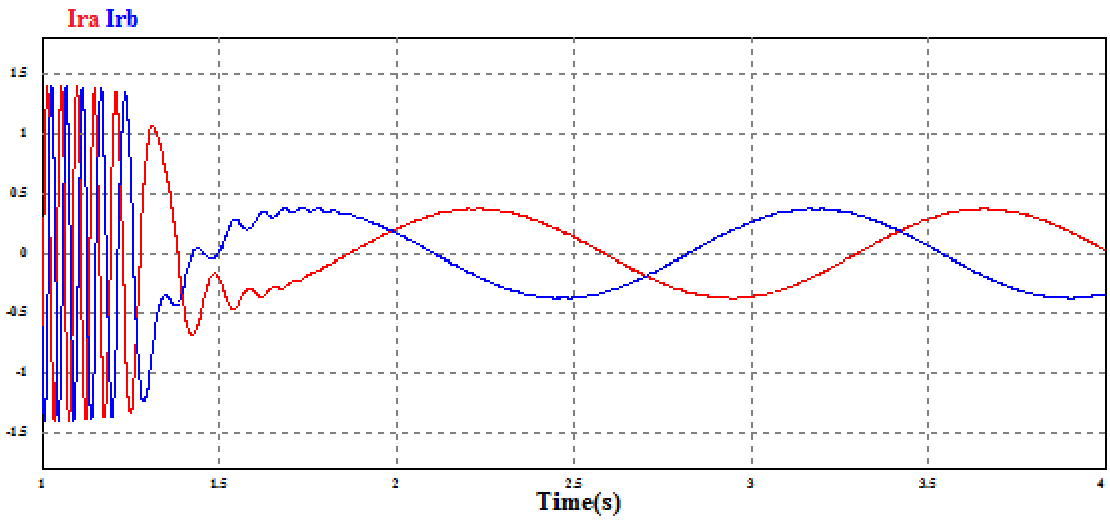

Figure 4.18: Rotor Current

Scale: current in A-phase(Red): X-axis: 1 Div=0.5 sec, Y-axis: 1 Div=0.5 pu.
current in B-phase (Blue): X-axis: 1 Div=0.5 sec, Y-axis: 1 Div=0.5pu.

Figure 4.13 and 4.15 shows the stator voltage and current are converted into d-q axes respectively. Magnitude of d-axis stator voltage is equal to the magnitude of stator voltage and q-axis stator voltage is zero as discussed earlier. Figure 4.17 shows the q-d axes stator flux. Where, d-axis stator flux is zero.
The rotor phase-A and phase-B currents, I_{ar} and I_{br}, are shown in the figure 4.18. The phase-A current I_{br} leads the phase-B current I_{ar} in the sub-synchronous mode, but the phase relation reverses in the super-synchronous mode. This is caused by the change in the slip, positive in the sub-synchronous mode and become negative value when the DFIG is in the super-synchronous mode.

Below Figure 4.19 and 4.20 shows the reference value (which is generated after the compering active and reactive power) and actual value of d-q axes rotor currents. Figure 4.21 shows the stator active power which is -1.5 pu and Figure 4.22 shows the stator reactive power which is zero.

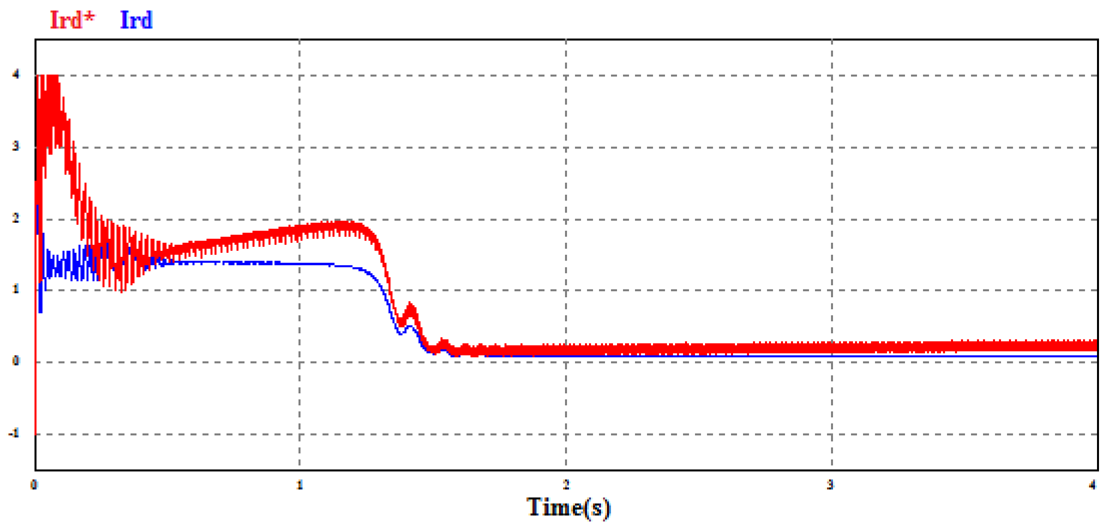

Figure 4.19: d-axis rotor current

Scale: reference d-axis current(Red): X-axis: 1 Div=1 sec, Y-axis: 1 Div=1 pu.
actual d-axis current (Blue): X-axis: 1 Div=1 sec, Y-axis: 1 Div=1 pu.

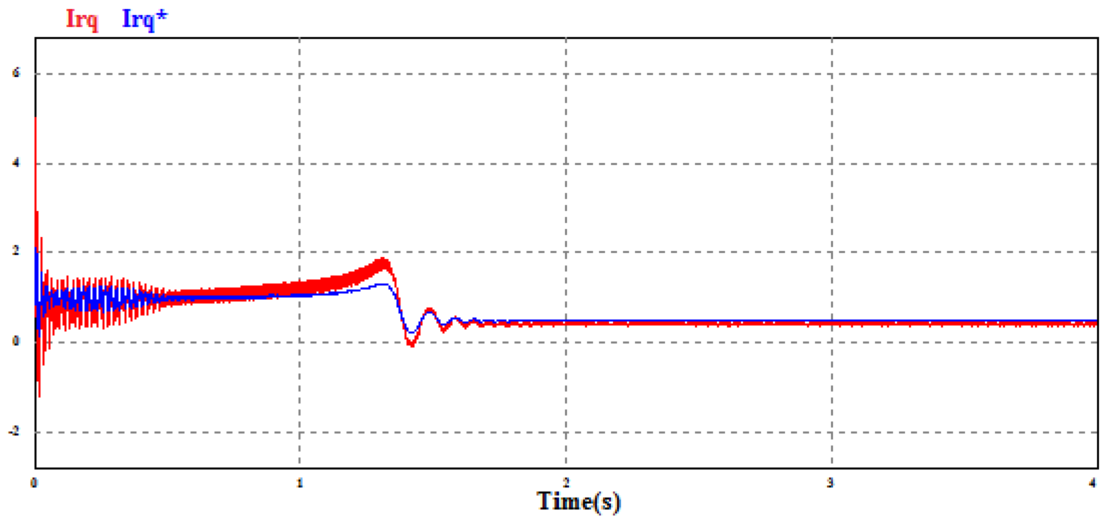

Figure 4.20: q-axis rotor current

Scale: reference q-axis current(Red): X-axis: 1 Div=1 sec, Y-axis: 1 Div=1 pu.
actual q-axis current (Blue): X-axis: 1 Div=1 sec, Y-axis: 1 Div=1 pu.

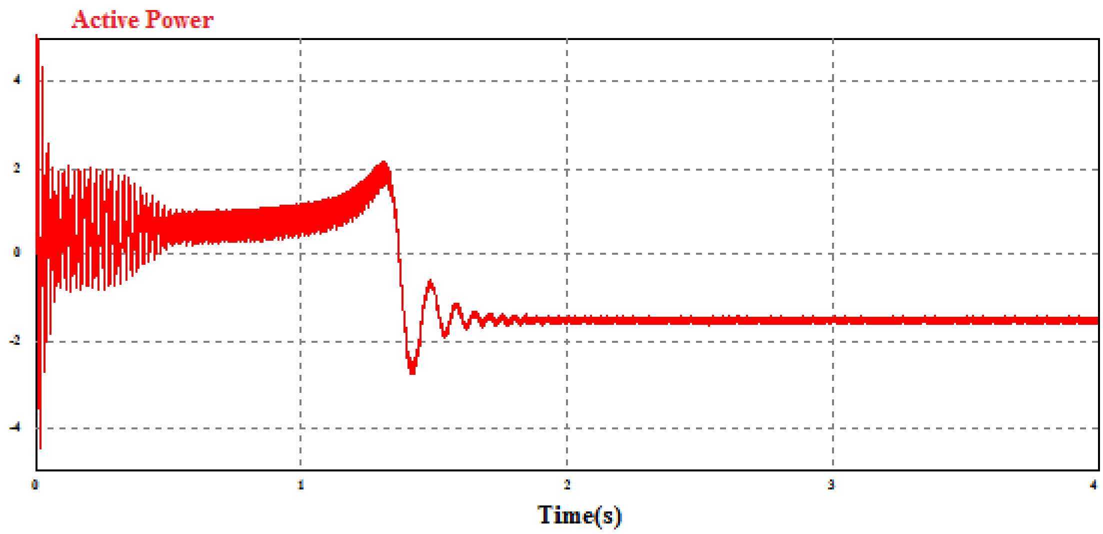

Figure 4.21: Stator Active power

Scale: Active Power: X-axis: 1 Div=1 sec, Y-axis: 1 Div=2 pu.

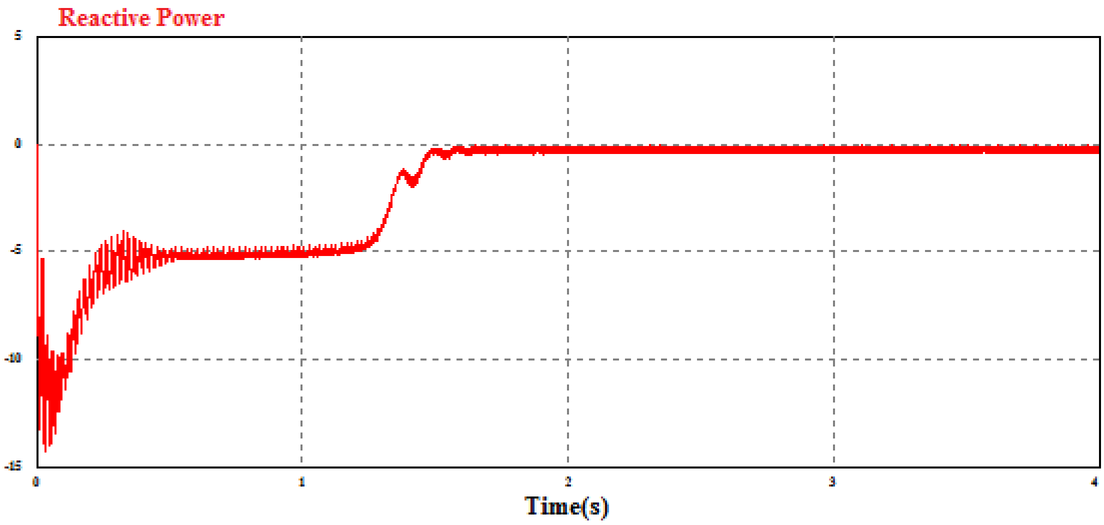

Figure 4.22: Stator reactive power

Scale: Reactive Power: X-axis: 1 Div=1 sec, Y-axis: 1 Div=2 pu.

4.2.2 Grid Side Converter Control

Figure 4.23 shows the control of Grid side converter which is simulated in PSIM. Figure 4.25 shows the 1000 V DC-link and it has 10 V ripple as shown in figure 4.26.

Figure 4.27 and 4.28 shows the reference value (which is generated after the compering DC-link voltage and reactive power) and actual value of d-q axes rotor currents. Figure 4.29 shows the power factor at grid side which is unity.

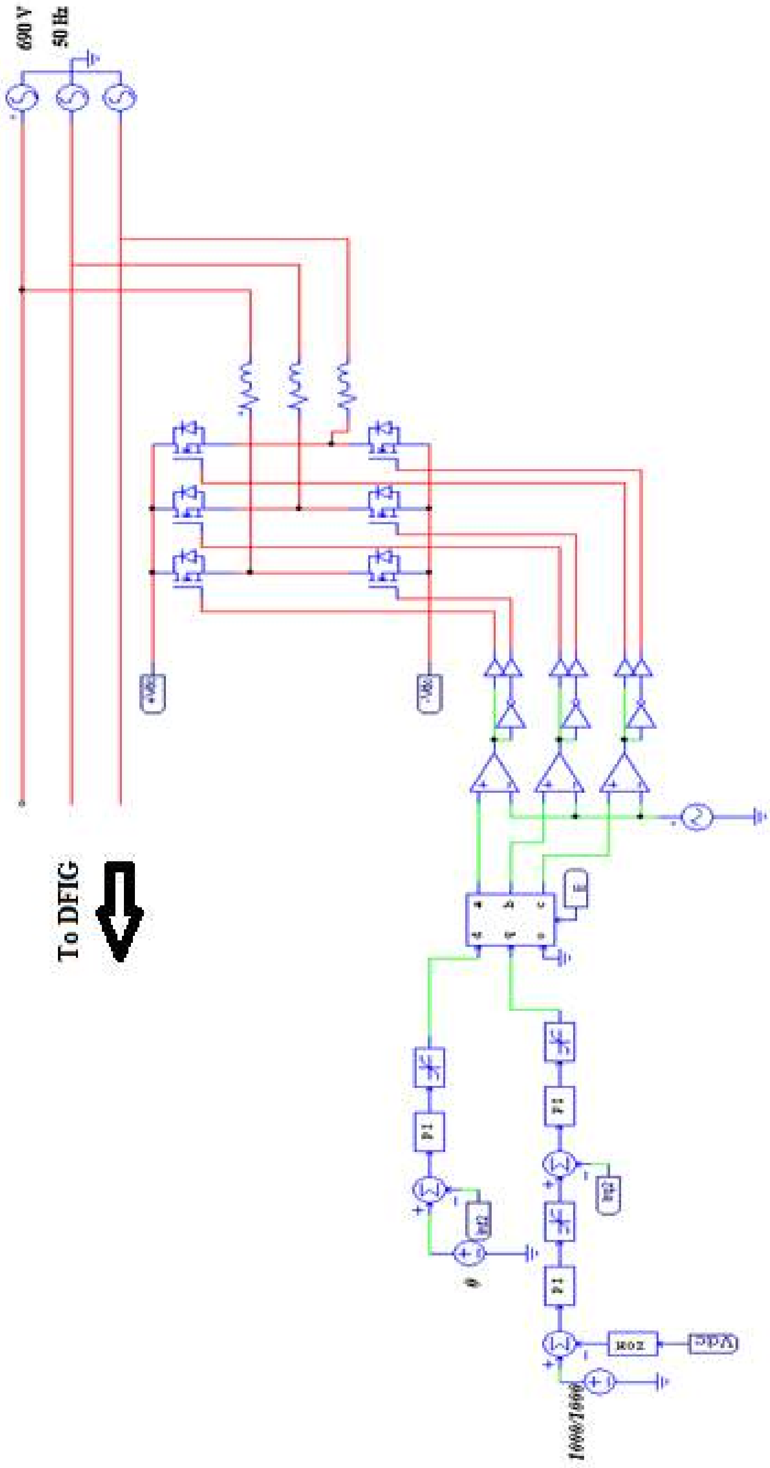

Figure 4.23: control for grid side converter

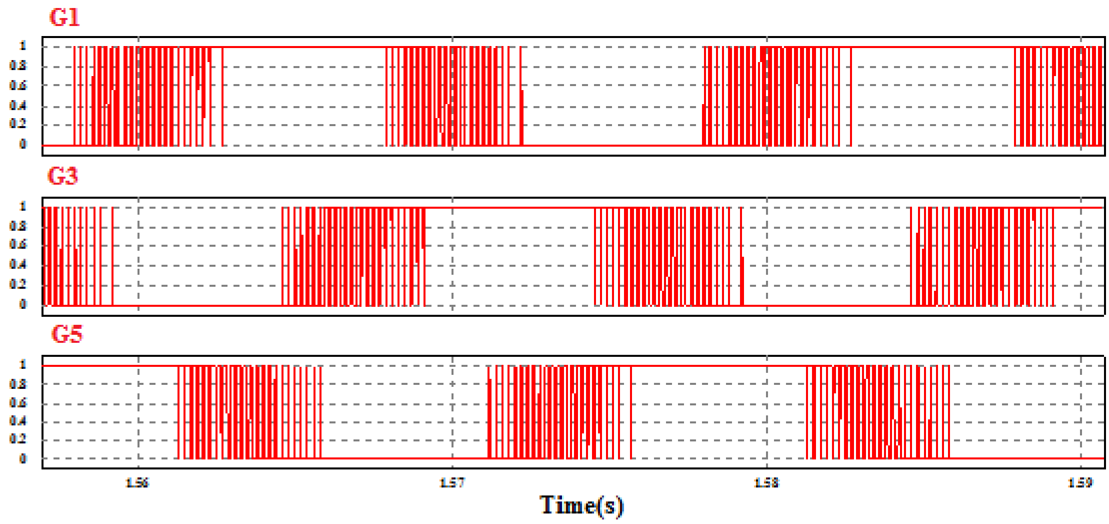

Figure 4.24: Gate pulse for switch S1, S3 and S5 of GSC

Scale: Gate pulse: X-axis: 1 Div=0.01 sec, Y-axis: 1 Div=1 V.

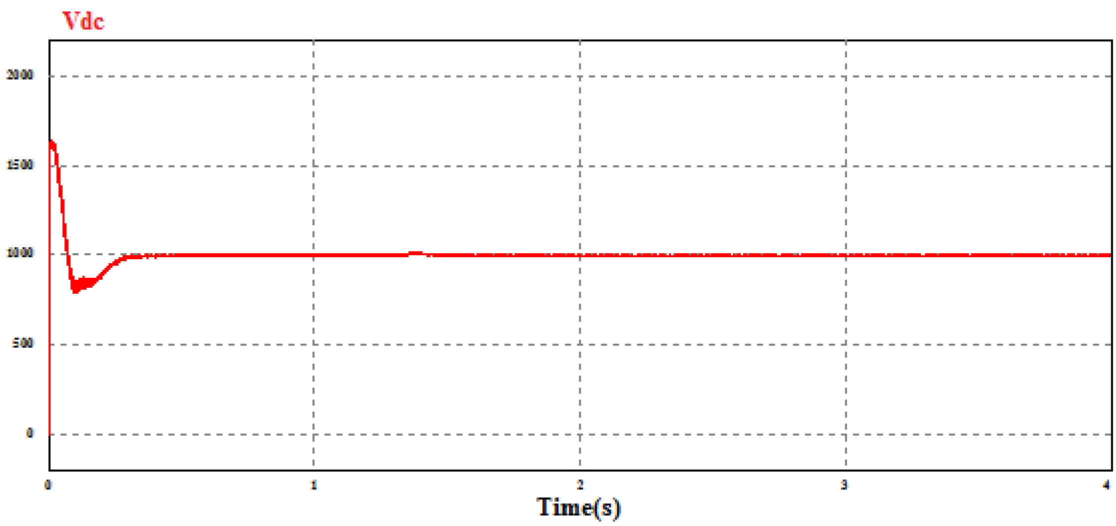

Figure 4.25: DC-link voltage

Scale: DC-link voltage: X-axis: 1 Div=1 sec, Y-axis: 1 Div=500 V.

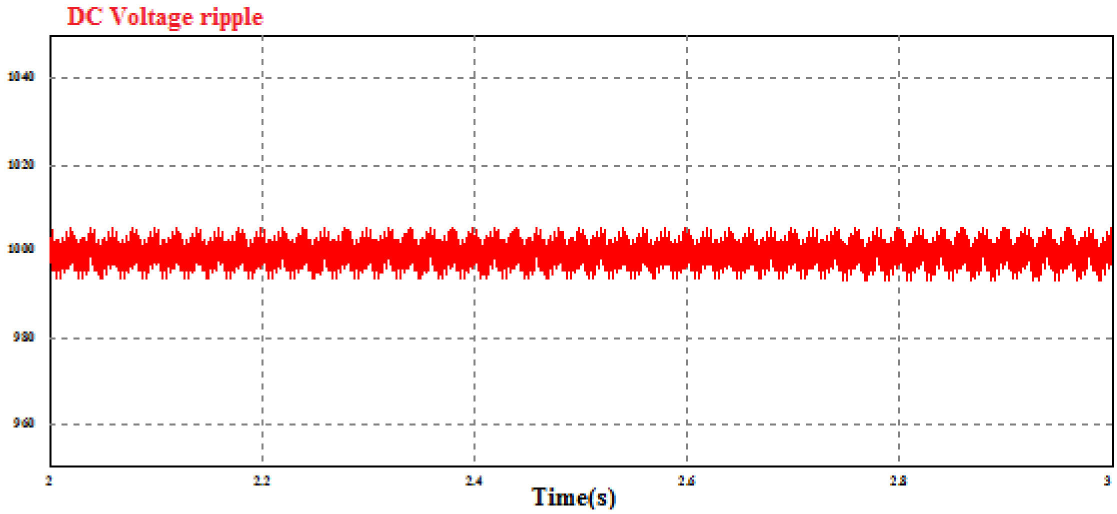

Figure 4.26: DC-link voltage ripple

Scale: DC-link voltage: X-axis: 1 Div=0.2 sec, Y-axis: 1 Div=20 V.

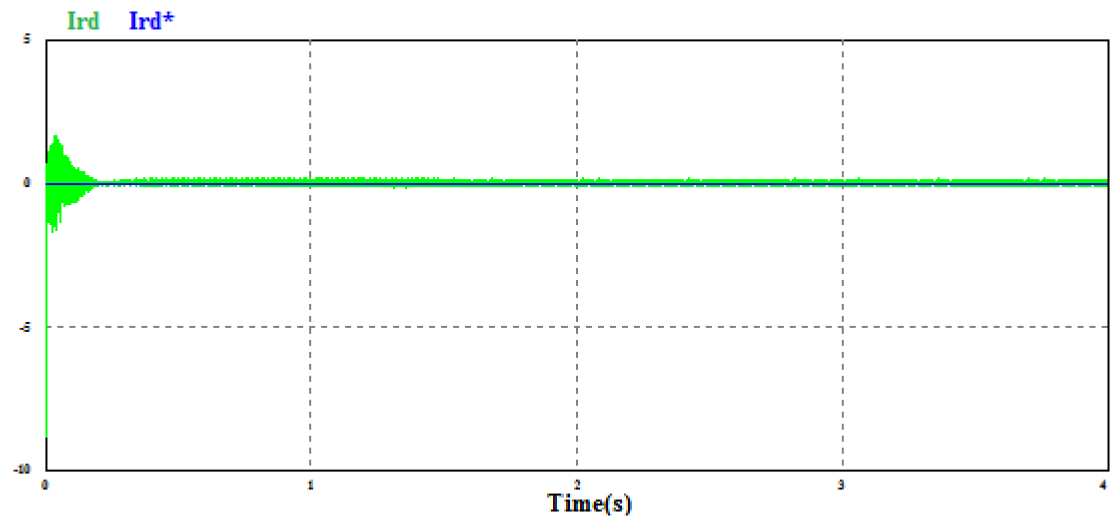

Figure 4.27: d-axis rotor current

Scale: reference d-axis current(Blue): X-axis: 1 Div=1 sec, Y-axis: 1 Div=5 pu.
actual d-axis current (Green): X-axis: 1 Div=1 sec, Y-axis: 1 Div=5 pu.

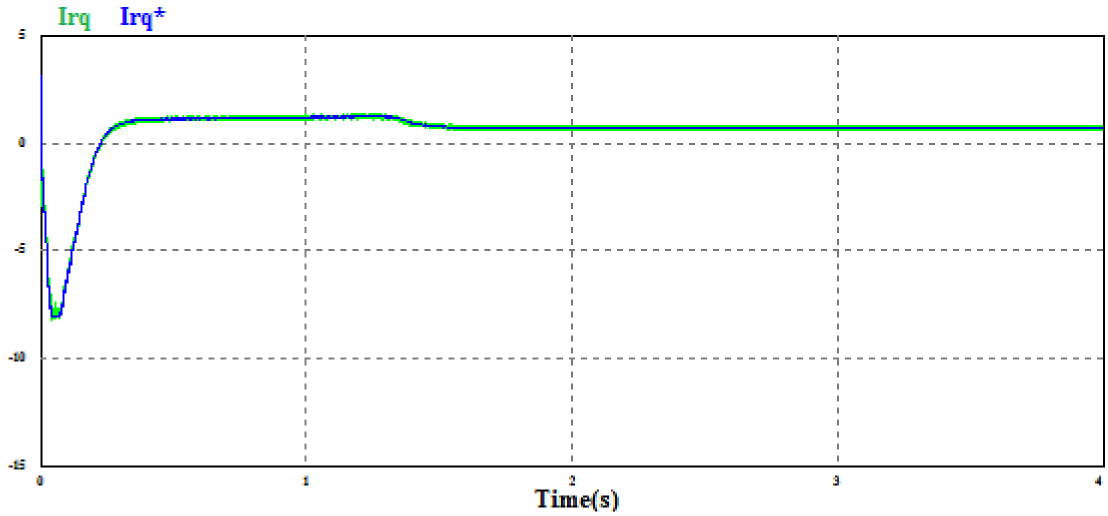

Figure 4.28: q-axis rotor current

Scale: reference q-axis current(Blue): X-axis: 1 Div=1 sec, Y-axis: 1 Div=5 pu. actual q-axis current (Green): X-axis: 1 Div=1 sec, Y-axis: 1 Div=5 pu.

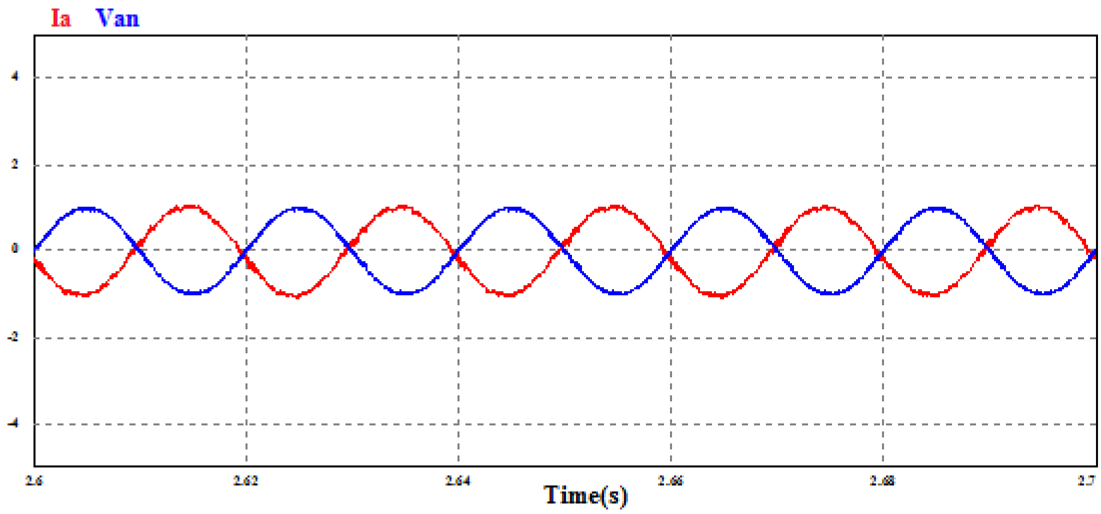

Figure 4.29: Power factor

Scale: current (red): X-axis: 1 Div=0.02 sec, Y-axis: 1 Div=2 pu. voltage (blue):X-axis: 1 Div=0.02 sec, Y-axis: 1 Div=2 pu.

4.3 DFIG parameter

Table II: DFIG parameter

Power	2 MW
Voltage	690 V
Rotor resistance	2.9 mΩ
stator leakage inductance	87 μH
Rotor leakage inductance	87 μH
magnetizing inductance	2.5 mH
No. of poles	4
frequency	50 Hz

Chapter 5

Conclusion

Doubly-Fed Induction Generator is widely used in the wind power industry to produce wind energy. Due to, the partial scale power converter the cost of converter and the hence the cost of system is less. The stator flux oriented vector control scheme is used to control the RSC and GSC. The aerodynamic model of wind turbine is simulated and the operation in MPPT mode and Pitch angle control mode is analyzed. The performance of DFIG is analyzed at the super-synchronous speed, the machine side converter provides good decoupling between active and reactive powers, and the grid side converter maintain DC-link voltage and power factor to be unity, which leads to high power quality and higher efficiency in harnessing wind energy effectively.

References

[1] "Global wind energy council 2013", international energy agency.

[2] "World Energy Outlook 2013, international energy agencies.

[3] G. A. Smith, K. Nigim, A. Smith, "Wind-energy recovery by a static Scherbius induction generator", IEE Proc., vol. 128, no.6, pp. 317-324, 1981.

[4] J. Marques, H. Pinheiro, et al., "A Survey On Variable-Speed Wind Turbine System", Federal University of Santa Maria.

[5] D. S. Zinger and E. Muljadi, "Annualized wind energy improvement using variable speeds", IEEE Trans. Ind. Application., vol. 33, no. 6, pp. 1444−1447, Nov./Dec. 1997.

[6] P. Mutschler and R. Hoffmann, "Comparison of wind turbines regarding their energy generation", in Proc. 2002 IEEE 33rd Annual IEEE Power Electronics Specialists Conference, vol. 1, Cairns, Qld., Australia, June, 2002, pp. 6−11.

[7] Rajib Datta and V. T. Ranganathan, "Variable-speed wind power generation using doubly fed wound rotor induction machine-a comparison with alternative schemes", IEEE Trans. Energy Conversion, vol. 17, no. 3, pp. 414−421, Sept. 2002.

[8] Deepak kumar, B. kumar, "Study of power generation of Doubly Fed Induction Generator in wind energy conversion system", ISSN: 2319−9598, Vol. 1, 2013.

[9] Janaka B. Ekanayake, Lee Holdsworth, XueGuang Wu, and Nicholas Jenkins, "Dynamic Modeling of Doubly Fed Induction Generator for Wind Turbines", IEEE transactions on power system, Vol. 18, No. 2, May 2003.

[10] P.C.Krause, "Analysis of electric machinary and drive system", 2nd edition, IEEE press.

[11] I. Boldea "Variable Speed Generator", CRC press, Boca Raton, 2006.

[12] B. Hopfensperger, D. J. Atkinson, and R. A. Lakin, "Stator-flux-oriented control of a doubly-fed induction machine with and without position encoder", IEE Proc. Electr. Power Appl., vol. 147, pp. 241−250, July 2000. W. Leonhard, Control of Electrical Drives, 2nd ed. Berlin, Germany: Springer- Verlag, 1996.

[13] W. Leonhard, Control of Electrical Drives, 2nd ed. Berlin, Germany: Springer-Verlag, 1996.

[14] R. Pena, J. C. Clare, and G. M. Asher, "Doubly fed induction generator using back-to-back PWM converters and its application to variable-speed wind-energy generation", IEE Proc. Electr. Power Appl., vol. 143, pp. 231−241, May 1996.

[15] YU Fang, LIU Qi-hui, ZHANG Jian-hua, "Flexible Grid-connection Technique and Novel Maximum Wind Power Tracking Algorithm for Doubly-Fed Wind Power Generator", The 33^{rd} Annual Conference of the IEEE Industrial Electronics Society (IECON). November 2007, Taipei, Taiwan.

[16] M.Yamamoto, and O. Motoyoshi, "Active and Reactive power Control for doubly-fed wound rotor induction generator", IEEE trans on PE-6,4,1991, pp 624−629.

[17] Y. Tang and L. Xu, "Flexible active and reactive power control strategy for a variable speed constant frequency generating system", IEEE Trans. Power Electron., vol. 10, no. 4, pp. 472−478, July 1995.

Appendix A

List of publication

- Chirag Vadaliya, Amit N Patel, Vinod Patel "Simulation on Stator Oriented Vector Controlled Doubly-Fed Induction Generator for Harnesseing Wind Energy Effectively", Paper will be publishing in International Conference On Advances In Engineering And Technology, which is going to be held at IIT Roorkee, INDIA during 24-25 May, 2014.